UNIVERSITY OF MANITOBA

A STRUCTURAL ANALYSIS OF THE SAN ANTONIO FORMATION, RICE LAKE AREA, MANITOBA

A DISSERTATION

SUBMITTED TO THE GRADUATE SCHOOL

IN PARTIAL FULFILLMENT OF THE REQUIREMENTS

for the degree

MASTER OF SCIENCE

by

ROGER JOSEPH RECTOR

WINNIPEG, MANITOBA

1966

Frontispiece

San Antonio Gold Mine-Bissett Manitoba

ABSTRACT

The San Antonio formation is a feldspathic quartzite which has been folded into an anticline - syncline pair. The limb common to both folds is overturned to the south. Mesoscopic data indicate that the syncline plunges to the east; macroscopic and mesoscopic data indicate that the anticline plunges to the northwest. The anticline appears to be a product of flexural slip folding followed by slip folding along the foliation plane.

A study of the microfabric reveals that the c-axes of the detrital quartz grains are preferentially orientated. Four maxima lie in two mutually perpendicular planes which contain "β_1" and are 45° from "a" and "c". The maxima also lie on the surface of a cone, the axis of which is "β_1". and the apical angle of which is 136°. This fabric is interpreted to be the preferential orientation of quartz along incipient S planes due to a compressive stress acting in the direction of the "a" geometric axis.

The formation has been folded above an unconformity surface which may have acted as a décollement. The intrusion of a potassic rich granite north of the San Antonio formation appears to have caused the formation to be thrust southward. The thrusting was accompanied by folding in the San Antonio formation.

Table of Contents

Page

Tables

ILLUSTRATIONS

Figures

Plates

Page

Page

CHAPTER I

INTRODUCTION

Statement of the Problem

The San Antonio formation is a clastic feldspathic quartzite which unconformably overlies the Rice Lake group of volcanic and sedimentary rocks in the Rice Lake area of Manitoba. The formation has been folded into an overturned anticlinal and synclinal pair. The objectives of this study are to determine the macroscopic, mesoscopic and microscopic fabric elements of the structure and to interpret the evolution of the development of the structure within the San Antonio formation.

Acknowledgements

The research for this thesis was carried out in the Department of Geology of the University of Manitoba during the 1963-64 academic year.

I wish to express my sincere gratitude to Professor W.C. Brisbin who not only suggested the problem but also provided guidance and assistance throughout the work.

I am also indebted to Dr. J.F. Davies of the Manitoba Mines Branch for the use of aerial photographs and the accompanying map and report on the Rice Lake area.

My thanks also go to the graduate students in the Department of Geology for their many stimulating discussions throughout the year.

The financial assistance provided by the Geological Survey of Canada is deeply appreciated.

Location and Access

The Rice Lake area is bounded by longitudes 95°30', 95°50' W and latitudes 50°57', 51°08' N and is approximately 100 air miles northeast of Winnipeg (Plate 1). The major community in the area is the gold mining town of Bissett. For years, access was gained by boats operating on Lake Winnipeg and the Wanipigow River, or by float plane from Lac Du Bonnet. Now, an all-weather road connects Bissett with Pine Falls, a community on the Winnipeg River at the end of Manitoba Highway No. 11.

Topographic Expression

The country around Rice Lake is typical of much of the Precambrian Shield. Rock outcrops form ridges with the characteristic appearance of a terrain which has undergone continental glaciation (Plate 2). Rock exposures and ridges are separated by areas of swamp and muskeg. Maximum relief rarely exceeds 100 feet. Geological investigation of the area is aided by numerous rock exposures and an absence of vegetation caused by fires in the past.

Drainage of the area is towards the west to Lake Winnipeg along the two major waterways, the Wanipigow and the Manigotagan rivers.

Previous Work

The earliest work in the area was done by Moore (1912), who conducted a reconnaissance survey along the main water routes east and south of Lake Winnipeg. Cooke (1921) made a detailed study around Rice Lake. Extensive mapping around Rice Lake as well as some of the surrounding terrain in southeastern Manitoba was carried out by Wright (1923, 1925, 1927, 1932).

Stockwell (1938) published the results of detailed mapping in the vic-

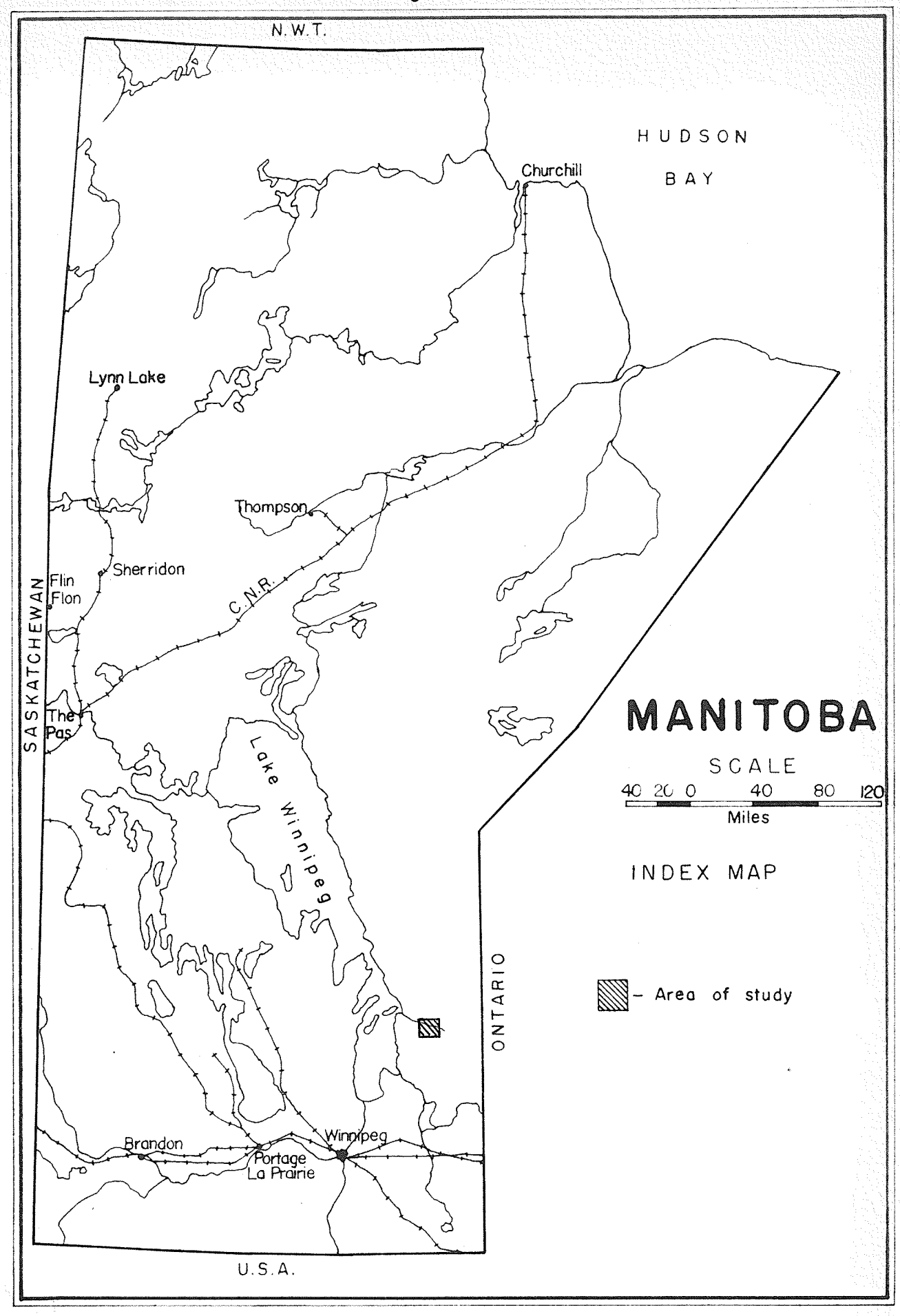
N.W.T.
HUDSON
BAY
Churchill
Lynn Lake
Thompson
Sherridon
Flin
Flon
C.N.R.
SASKATCHEWAN
The
Pas
Lake Winnipeg
ONTARIO
MANITOBA
SCALE
40 20 0 40 80 120
Miles
INDEX MAP
- Area of study
Brandon
Portage
La Prairie
Winnipeg
U.S.A.

PLATE I

Glaciated outcrop of San Antonio Formation. Outcrop west of Horseshoe Lake.

Plate-2

inity of the San Antonio Mine. He made an important contribution to the understanding of the stratigraphy and the structural geology of the Rice Lake area by recognizing that the sedimentary rocks east of Rice Lake were interbedded with the volcanic rocks, while those west of Rice Lake unconformably overlay the interbedded volcanic and sedimentary rocks as well as a body of quartz diorite. These younger rocks were named the "San Antonio formation" (Stockwell 1938).

Stanton (1941) conducted a heavy mineral study of the San Antonio formation and the surrounding intrusive rocks. On the basis of the zircons found in the San Antonio formation and in the intrusive rocks he concluded that the formation was younger than all of the surrounding intrusive rocks.

In later field work Stockwell (1945) determined that the San Antonio formation overlay the quartzose sediments of the Wanipigow River area.

Further work was done by Davies (1949, 1950, 1953, and 1963). The last of Davies' work (1963) considers the regional structural geology of the Rice Lake area and especially the relationship of the San Antonio formation to the Rice Lake group.

CHAPTER 2

GEOLOGY

General Statement

The general geology in this section is based primarily on the work of Davies (1963). Some additional new information is provided by the writer in the section dealing with the geology of the San Antonio formation.

General Geology

The consolidated rocks of the area are all Precambrian in age. The Rice Lake area lies in a belt of meta-volcanic and associated meta-sedimentary rocks extending from the mouth of the Wanipigow River to the Ontario boundary. In Manitoba this belt is approximately 60 miles long and varies in width from 1 to 15 miles. In the Rice Lake area, it is approximately 6 miles wide.

The geology in the immediate area of Rice Lake is illustrated on the accompanying map (Fig. 6, in the pocket). A Table of Formations is given in Table I.

In the vicinity of Rice Lake, the volcanic and sedimentary rocks of the Rice Lake group are intruded by a number of calcic intrusions. The San Antonio formation unconformably overlies both the Rice Lake group and the calcic intrusions but is older than the granitic rocks lying to the north (Davies, 1963). The San Antonio formation is not intruded by younger rocks except for some quartz veins of uncertain origin.

The Rice Lake group consists predominantly of volcanic ejecta material of acid to intermediate composition. Sedimentary rocks of the Rice Lake group are interbedded with and conformably overlie the volcanic rocks. Greywacke, subgreywacke and quartz-feldspar-mica gneiss are the dominant sedimentary types.

The calcic intrusions of gabbro, diabase, quartz diorite and quartz-feldspar porphyry are confined to the areas of volcanic rocks and appear genetically related to them (Davies, 1963).

TABLE I

Table of Formations

(After Davies, 1963)

Potassic Intrusions	Granite, granodiorite quartz diorite
Intrusive Contact	
San Antonio Formation	Feldspathic quartzite, conglomerate
Unconformity	
Calcic Intrusive Rocks	Peridotite, Quartz-feldspar porphyry Quartz diorite "Quartz eye granite" Diabase Gabbro
Intrusive Contact	
Rice Lake Group	Quartz-biotite-feldspar schist and gneiss Subgreywacke, greywacke, slate Dacite breccia, trachyte breccia Porphyritic dacite Dacite crystal tuff Basalt, chlorite schist Bedded tuff, lapilli tuff, arkose, conglomerate Rhyolite Porphyritic dacite breccia

Precambrian

The San Antonio formation consists of feldspathic quartzite and conglomerate. It unconformably overlies the rocks of the Rice Lake group and their associated intrusions.

The rocks of the Rice Lake group have been folded into a broad anticline, the axial trace of which lies 1/2 mile south of Rice Lake (Stockwell, 1945). The San Antonio formation has been folded into an anticlinal-synclinal pair overturned to the south. Folding in the San Antonio formation is not reflected in the underlying Rice Lake group (Davies, 1963).

Two fault directions predominate in the Rice Lake group: (1) northwest, and (2) east to northeast. Some of these faults are apparently occupied by later intrusive material forming dikes.

Mineral exploration in the area has been confined to the search for gold which occurs in quartz veins. A number of gold prospects have been thoroughly explored; these include the Packsack, Vanson, Wingold, Goldpan, Gold Lake, Poundmaker, Jeep and the San Antonio. Of these only the San Antonio (frontispiece) is still a producing mine.

Glacial deposits consist of glacial till, some lacustrine clays, and some small scattered deposits of sand and gravel. Glacial striae, well preserved on many outcrops, strike south 60° west.

Geology of the San Antonio Formation

Occurrence and Distribution

The principal outcrop area of the formation is west of Horseshoe Lake and Rice Lake, and around Little Rice Lake. The outcrop pattern is in the form of an irregular S. One narrow discontinuous band extends along the northern edge of a body of quartz diorite.

Sedimentary Structures

Normal bedding is not well developed in much of the formation. Bedding is

especially difficult to observe in the central portion of the formation where very little argillaceous material is present to mark the bedding surfaces. Bedding is revealed by wisps of argillaceous material, beds and lenses of conglomerate, graded bedding, and the boundaries of successive cross-beds. In the southern portion of the formation, argillaceous material is relatively abundant, and bedding is easily observed (Plate 3A).

The San Antonio formation has locally abundant cross-bedding (Plate 4) and graded bedding, both of which provide useful top determinations. Cross-beds vary in length from two to fifteen feet. Graded bedding is much less common but does occur erratically throughout the formation (Plate 3B). Some scour and fill structures also occur.

Red Beds

A distinct area of red beds covers much of the central portion of the formation. The distribution of the red beds, based on a brief field examination, is given in Figure 1. The red beds are pink to brownish red in colour (Plate 5A, B). The red beds are predominantly coarse feldspathic quartzite with very little argillaceous material. A few scattered lenses and beds of conglomerate occur in the red beds. The pebbles are composed of quartz, rhyolite, green schist, jasper and some feldspar porphyry.

A continuous but patchy zone of conglomerate, 10 to 75 feet thick occurs 3,000 feet west of Horseshoe Lake. This zone forms a useful marker horizon in the area. Pebbles and a few boulders in this conglomerate represent a variable source terrain. The pebbles are composed of white quartz, jasper, rhyolite, granite, green schist, basalt and feldspar porphyry. The fragments vary from 1/2 to 6 inches across and show considerable variation in the degree of deformation. Intense shearing has obliterated the rounding of many of the fragments.

A. Normal bedding - Gold Creek.

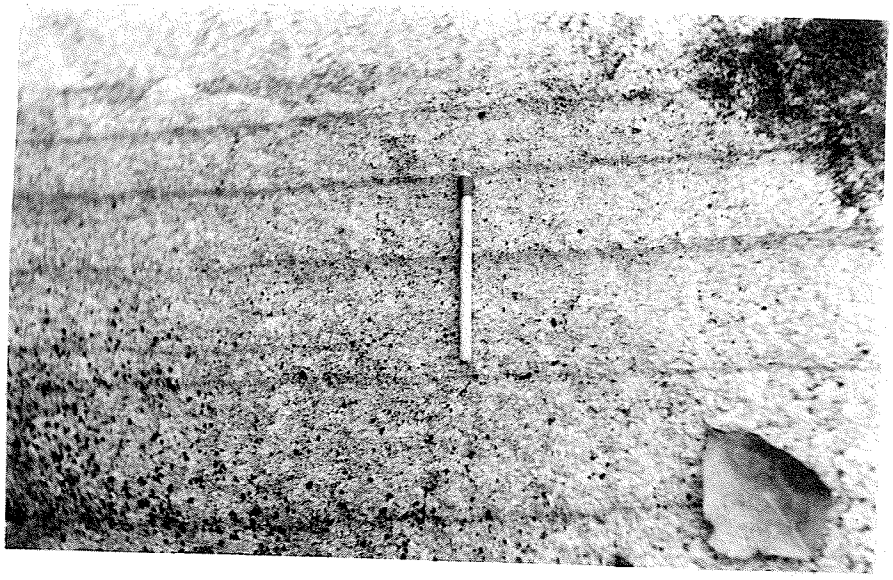

B. Graded bedding - Caribou Lake Road.

Plate - 3

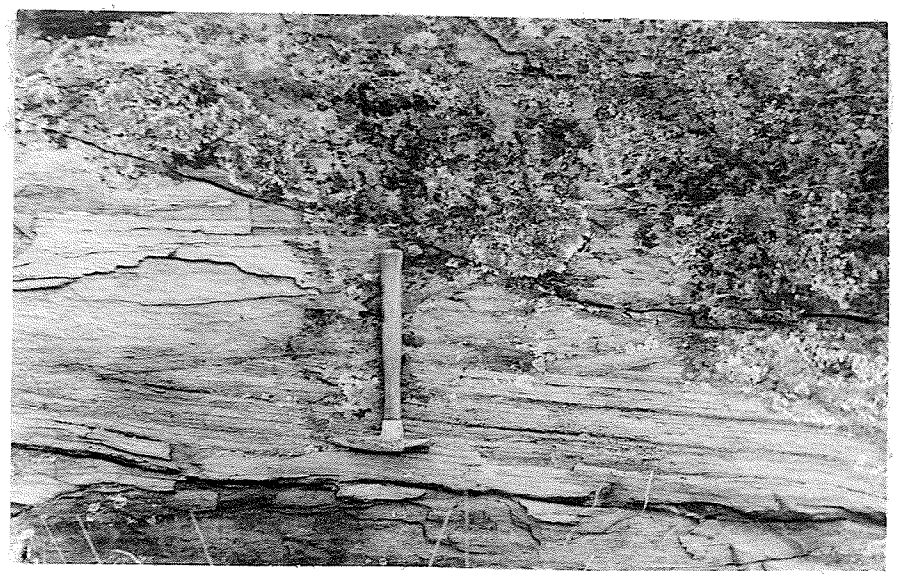

A. Cross-bedding - Gold Creek.

B. Cross-bedding - Caribou Lake Road.

Plate - 4

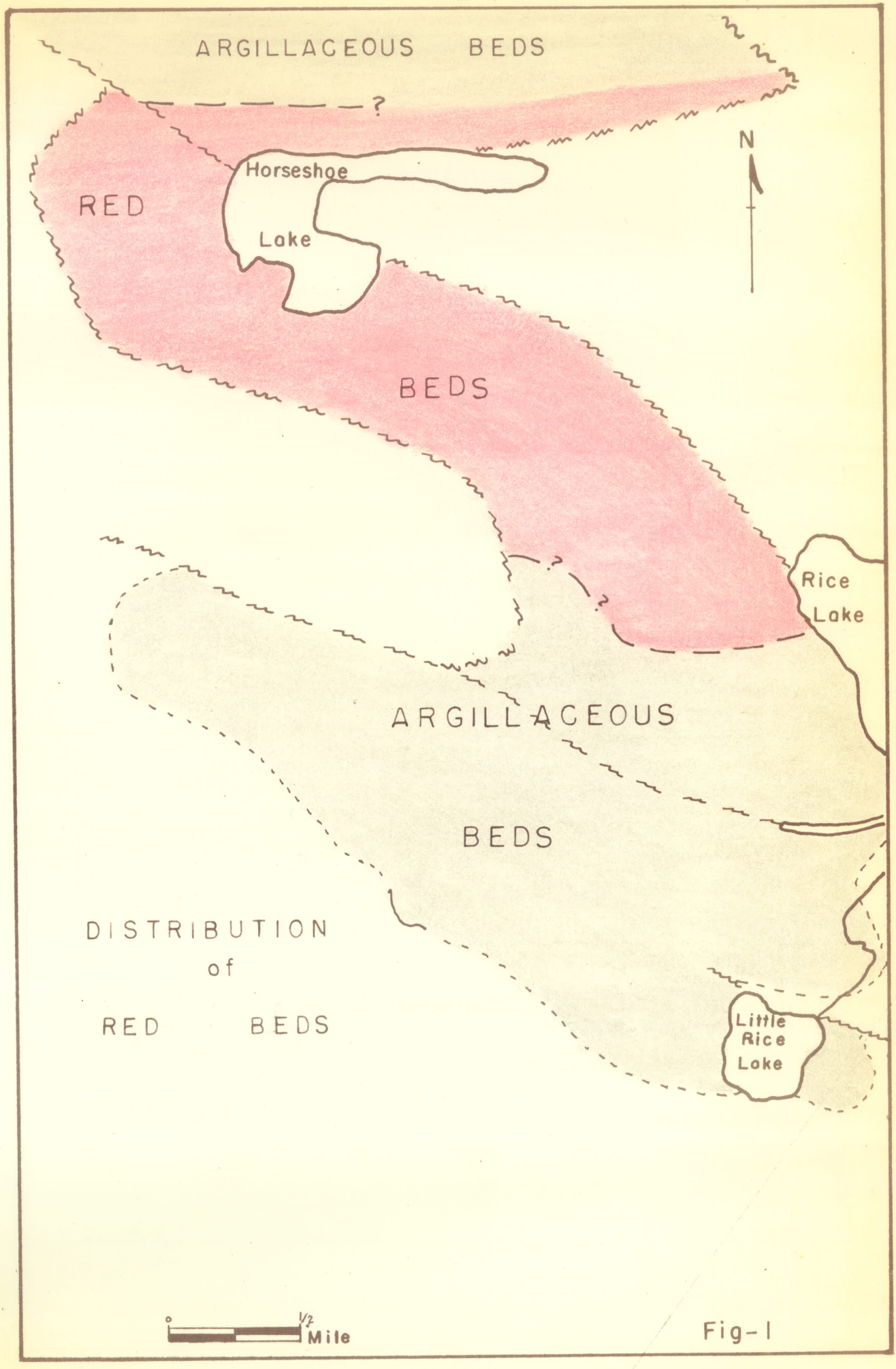
ARGILLACEOUS BEDS
?
N
Horseshoe
Lake
RED
BEDS
Rice
Lake
ARGILLACEOUS
BEDS
DISTRIBUTION
of
RED BEDS
Little
Rice
Lake
0
½
Mile

Fig-1

A. Red beds-outcrop west of Horseshoe Lake.

B. Cross-bedding in red beds-outcrop west of Horseshoe Lake.

Plate - 5

In thin section, the quartzite from the red beds is characterized by large distinct grains of highly strained quartz and feldspar; the grains are separated by fine interstitial material (Plate 6A). The quartz is largely unrecrystallized; recrystallization is mainly confined to the borders of grains and healed fractures. Generally, the quartz has a rounded to elliptical form and is not highly fractured. Deformation lamellae, undulose bands, and some mylonitized quartz have been identified in some thin sections. The feldspar grains are commonly fractured and have undergone various degrees of sericitization. Microcline is the dominant feldspar present in the red beds. Sericite, chlorite, and in some areas crushed quartz and feldspar form the matrix. The red colour of the San Antonio formation is due to disseminations of fine red hematite. Minor amounts of detrital zircon and secondary calcite occur in some areas.

Argillaceous Beds

The so-called argillaceous beds of the San Antonio formation outcrop in the southern portion of the formation and also north of Horseshoe Lake (Figure 1). These beds are in fact psammitic, however they do contain more pelitic material than the red beds. The argillaceous beds vary from medium grey to brownish grey in colour. Bedding is quite distinct due to the argillaceous content (Plate 3A). Except for the basal conglomerate found at the southern edge of the formation, the argillaceous beds contain fewer pebbles than the red beds.

In the argillaceous beds the quartz has been to a large extent recrystallized (Plate 6B). The recrystallized grains have a straight extinction, whereas the unrecrystallized whole and remnant grains have an undulose extinction. The degree of strain exhibited by the unrecrystallized quartz in the argillaceous beds appears to be considerably less than in the red beds. The matrix in the argillaceous beds is predominantly chlorite. The common potash feldspar present

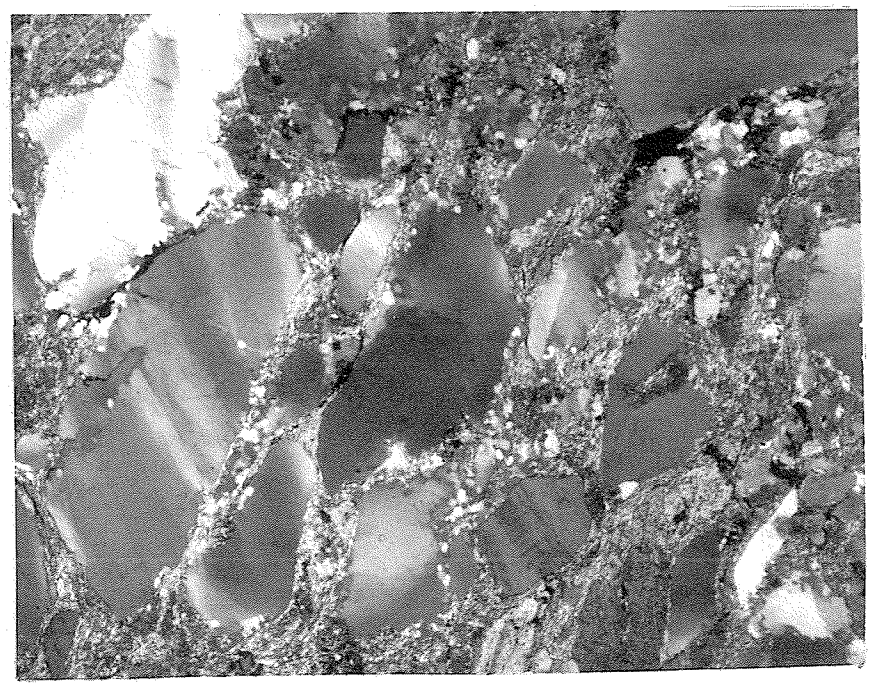

A. Unrecrystallized, highly strained quartz grains from red beds, crossed nicols, magnification 52X.

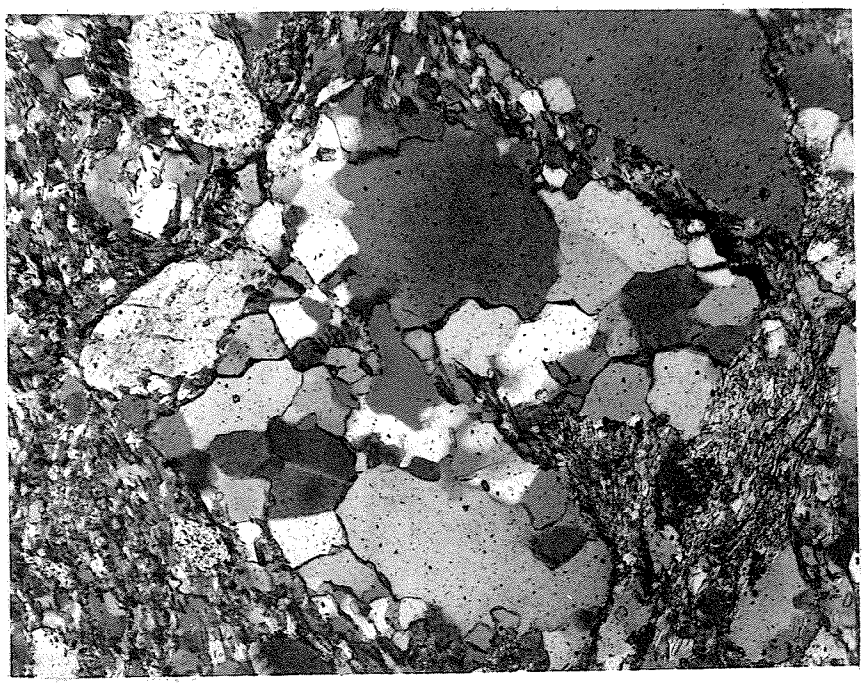

B. Recrystallized and partially recrystallized quartz grains from argillaceous beds, crossed nicols, magnification 70X.

Plate 6.

in the argillaceous beds is orthoclase. Accessory minerals are hematite, epidote, detrital zircon and secondary calcite.

Basal Conglomerate and Unconformity Features

A basal conglomerate exposed beside a small lake on the isolated southern arm of the San Antonio formation (Figure 6) varies in thickness from 10 feet or less to 80 feet. Davies (1963, p. 65) describes the conglomerate as containing:

> "abundant round to ellipsoidal pebbles, cobbles, and boulders of quartz diorite, light colored porphyritic lava and a few white quartz. Most of the fragments are cobbles 3 or 4 inches across; others are pebbles about an inch in diameter. However, boulders several feet across are present. The larger fragments are mostly quartz diorite identical to that on which the conglomerate lies. Pebbles, cobbles, and boulders make up about 50 per cent of the rock; the matrix is arkosic material."

At the same location the conglomerate - quartz diorite contact is irregular but sharp. Quartz veins in the quartz diorite abruptly terminate at the unconformity (Plate 7A).

Stockwell (1945) reports boulders up to 40 feet long and 20 feet wide in this basal conglomerate.

At the southeast end of Little Rice Lake, a coarse grit and conglomerate overlie the quartz diorite. What appears to be a "regolith" horizon has been preserved in the quartz diorite (Plate 7B); cracks in the quartz diorite are filled by coarse grit. Similarity between the quartz diorite and the grit gives rise to a so-called "gradational unconformity". The blue opalescent quartz grains, which characterize the quartz diorite are more abundant in the grit. The coarse grit forms a narrow zone along the contact of the quartz diorite.

One and a half miles east of Little Rice Lake the San Antonio formation and a porphyritic dacite breccia are in contact (Davies, 1963). At this location, the strike of the quartzite and the quartzite-breccia contact are perpendicular to

A. Unconformity between San Antonio formation and quartz diorite. Note abrupt termination of quartz veins at contact. (photo after Davies (1963)).

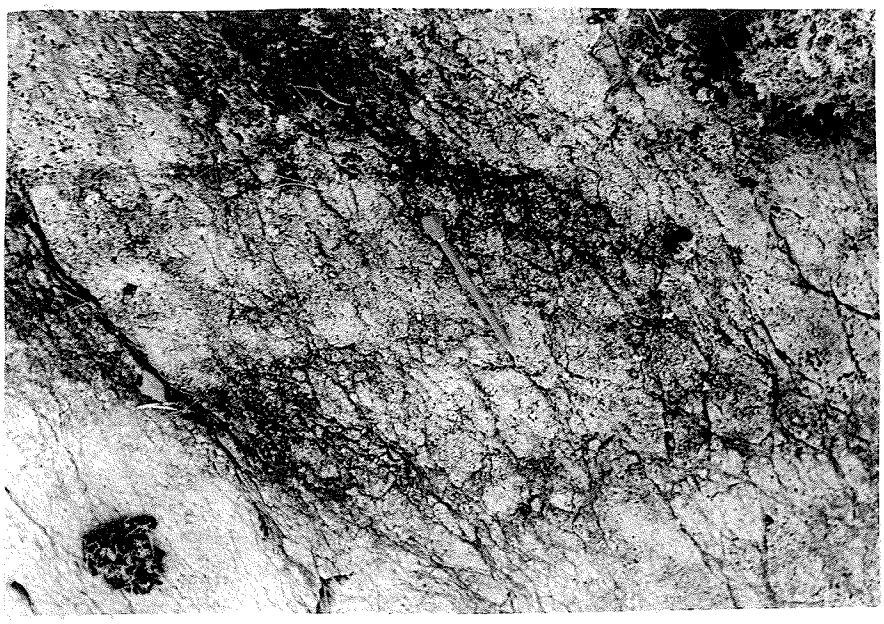

B. Plan view of an interpreted regolith horizon in quartz diorite - Little Rice Lake.

Plate - 7

the attitude of the breccia band (Davies, 1963). There is no evidence of faulting at this point.

One and a half miles west of Little Rice Lake, the quartzite is in contact with volcanic rocks. The volcanic rocks have been intruded by both quartz diorite and quartz-feldspar porphyry and show evidence of granitization. The quartzite is not intruded by either of these intrusive rocks, nor does it show any signs of granitization (Davies, 1963).

Faulting

The major occurrence of faulting in the San Antonio formation is found at the contact of the formation with the underlying Rice Lake group. South and west of Horseshoe Lake, strong shearing occurs around the nose of the anticlinal structure. The shearing dips beneath the San Antonio formation at 60° to 70° and marks the contact between the formation and the Rice Lake group. At this location the beds face west, and if projected to depth would apparently underlie the lavas of the Rice Lake group; however, this anomalous relationship is due to the aforementioned faulting.

A number of topographic lineaments observed on air photographs were examined in the field for evidence of faulting. Most of the outcrops along the lineaments were rounded by glaciation and have also undergone exfoliation. A freshly blasted road cut in the outcrop south of Horseshoe Lake revealed several surfaces of movement, the most prominent being a small shallow thrust fault, the sense of movement having been identified by slickensides. The thrust fault has a strike of N65°E and dips 40° to the northwest. Except for the blasted exposure, the thrust could not be observed. If other lineaments are faults of the same nature as the one at Horseshoe Lake, the shallow dip of the fault coupled with glaciation

and exfoliation of the outcrops would lessen the chances for the preservation of any features diagnostic of the faults. Most of the lineaments trend from N65°E to N90°E (Figure 2) and are parallel to known faults and shear zones. A lineament trending N70°W along Gold Creek is approximately parallel to the strike of the synclinal axial plane.

Structural Relationship to the Intrusive Rocks

Stockwell (1938) recognized the unconformable relationship of the San Antonio formation to the Rice Lake group. From heavy mineral studies of the San Antonio formation, Stanton (1941) concluded that it was younger than all the intrusions in the area. Although Wright (1932) believed that the San Antonio formation was intruded by granite, both Stockwell (1938) and Davies (1963) failed to find the field evidence on which Wright based his hypothesis.

Davies (1963) postulated that the granite intrusion north of the San Antonio formation was younger than the formation. He noted that the formation contained, at a maximum, only 10 percent microcline, which could have been derived from a potassic phase of the older dominantly calcic intrusions. The fact that Stanton (1941) found zircons characteristic of both calcic and potassic intrusive rocks in the San Antonio formation could also be accounted for by a potassic phase of the calcic intrusions. Age determinations (Lowdon, 1961) indicate that 800 million years elapsed between the orogenies producing the earlier calcic and the later potassic intrusions. This time interval may be considered sufficiently long to expose the calcic intrusions as a source area for the San Antonio formation (Davies, 1963).

Davies (1963) states that the structures of the San Antonio formation are not reflected in the Rice Lake group and similarily, the major anticline of the

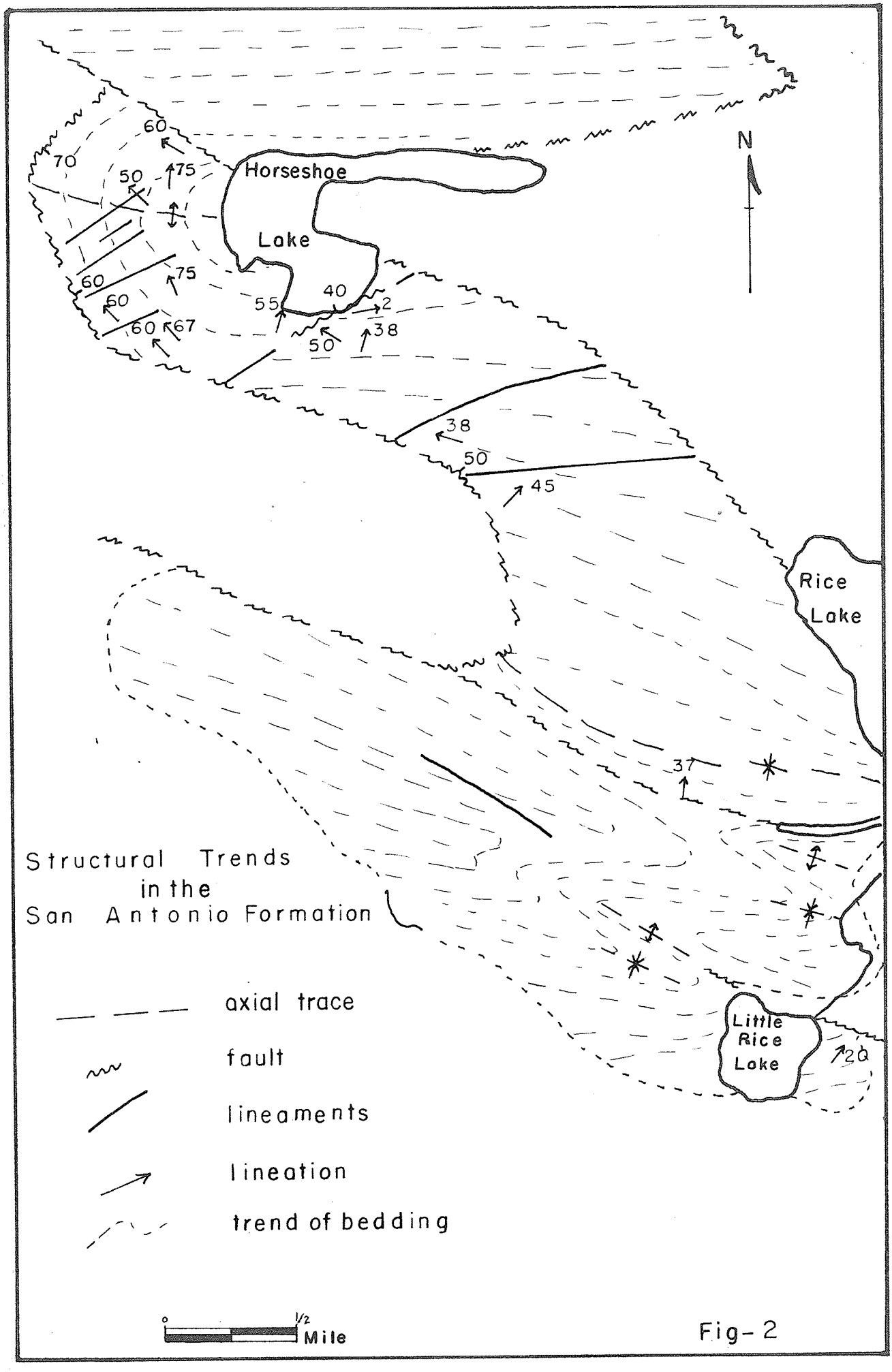
N
Horseshoe
Lake
Rice
Lake
Little
Rice
Lake
60
70
50
75
60
75
60
60
60
67
55
40
2
50
38
38
50
45
37
20
Structural Trends
in the
San Antonio Formation
axial trace
fault
lineaments
lineation
trend of bedding
0
1/2
Mile

Fig-2

Rice Lake group is not imposed on the San Antonio formation. He also postulates that the San Antonio formation had been thrust southward over the Rice Lake group. The quartz diorite appears to have acted as a buttress, and the intrusion of the potassic granite provided the force for the thrusting (Davies, 1963). This being the case, the unconformity acted as a décollement surface; the faulting found along the contacts of the formation is thus explained.

CHAPTER 3

DESCRIPTION AND INTERPRETATION OF MESOSCOPIC DATA

General Statement

The present work consists of a structural study of the main synclinal and anticlinal structures of the San Antonio formation. A total of five days was spent in the field in the spring and fall of 1963. The objectives of the field work were threefold: (1) collection of specimens for laboratory study, (2) collection of mesoscopic data, and (3) examination of critical outcrops delineating the major structures of the formation.

Mesoscopic structures were generally lacking or were poorly developed in much of the San Antonio formation. The prominent features on any outcrop were bedding, foliation and joints. Lineations were scarce and were primarily slickensides. All mesoscopic data were plotted and analyzed on a Schmidt equal area net. The data used in the analysis were collected by the author and supplemented by information from Stockwell (1938, 1945) and Davies (1949, 1950, 1953, 1963).

Bedding

Normal bedding, as previously mentioned, was often difficult to ascertain. Where bedding was observed, it formed a feature important to the structural interpretation of the San Antonio formation.

To analyze the bedding plane information the San Antonio formation was divided into two subareas (Figure 3). Subarea II, immediately west of Horseshoe Lake was isolated because of the structural complexities noted in the field. The area north of Horseshoe Lake is a structurally uncomplicated limb and is

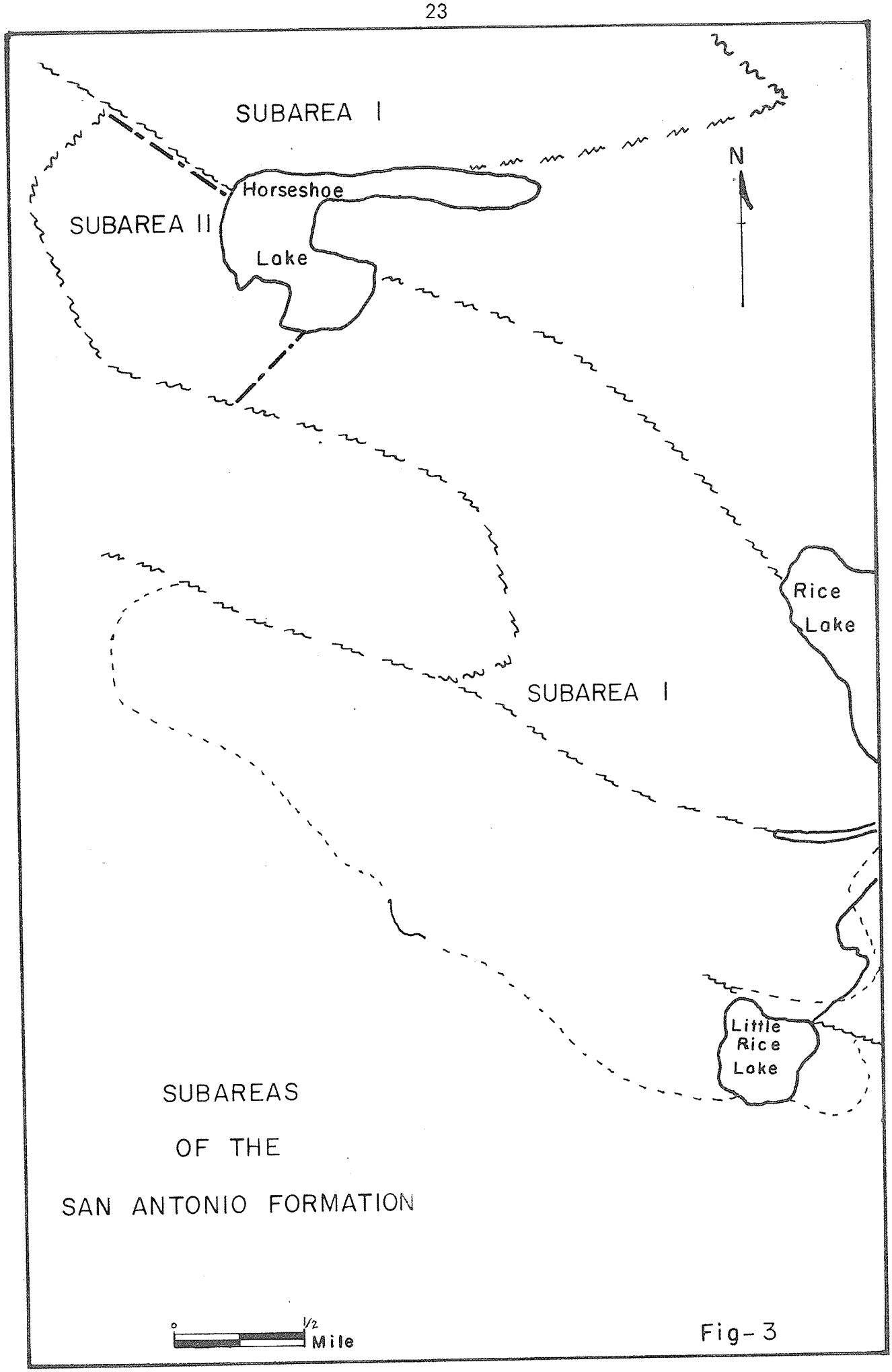
SUBAREA I
N
Horseshoe
SUBAREA II
Lake
Rice
Lake
SUBAREA I
Little
Rice
Lake
SUBAREAS
OF THE
SAN ANTONIO FORMATION
0
1/2
Mile

Fig-3

therefore included as a part of Subarea I.

Subarea I

The fabric diagram produced from a plot of the poles to the bedding from Subarea I (Plate 8A) shows the development of two well-defined maxima. One maximum lies close to the periphery of the net, and the other lies on a great circle about 50° from the periphery. The two maxima and the weakly developed girdle joining them form a segment of a great circle.

These maxima are interpreted as concentrations produced by limbs of an overturned fold (Dahlstrom, 1954). The pole to the great circle containing the maxima is "β_1", the statistical plunge of the synclinal fold. The plane which contains "β_1" and symmetrically bisects the fold is, by definition, the axial plane of the fold. The axial plane does not pass through the girdle joining the two maxima in Plate 8A because the fold is overturned. The fold plunges 16°/S85°E, and has an axial plane the attitude of which is N72°W/55°NE. A right section of the major synclinal fold in the San Antonio formation is constructed in Plate 9.

Subarea II

The geological map west of Horseshoe Lake indicates that the apparent plunge of the anticlinal fold is not to the east but to the west. Bedding in Subarea II is poorly defined and a local statistical analysis on the Schmidt net is not possible. However, from available bedding plane information a pole circle can be drawn and a plunge determined (Plate 8B). The data suggests that the anticline plunges 70°/N15°W, a direction considerably different to that of the syncline.

Foliation

Foliation forms the second most prominent mesoscopic feature. Folia-

A. Subarea I

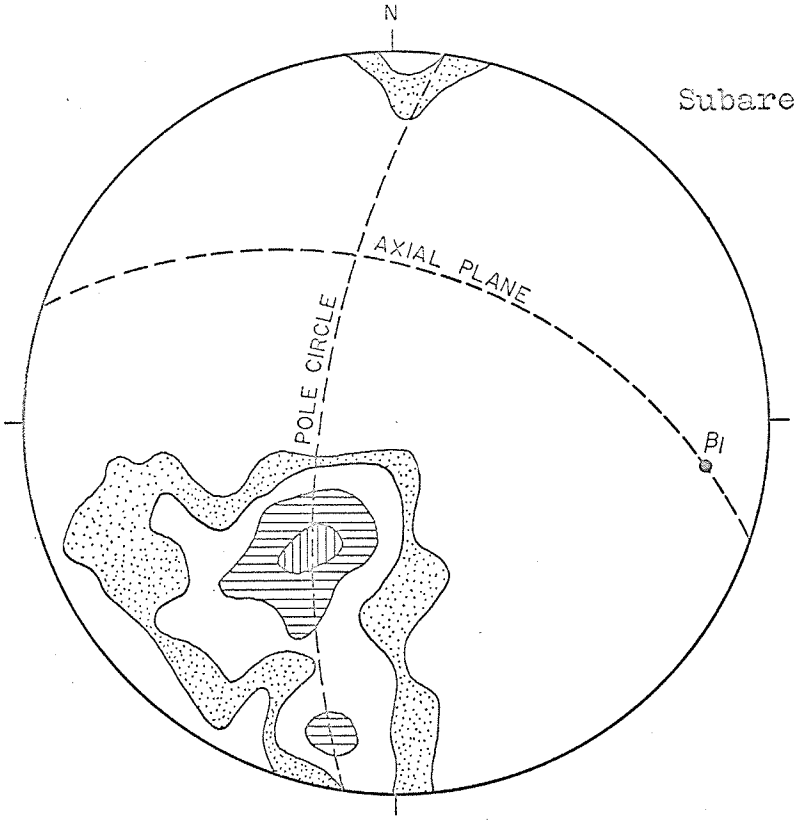

149 poles to bedding.

Contours: 1,3,8,15%
Max. 16.1%

B. Subarea II

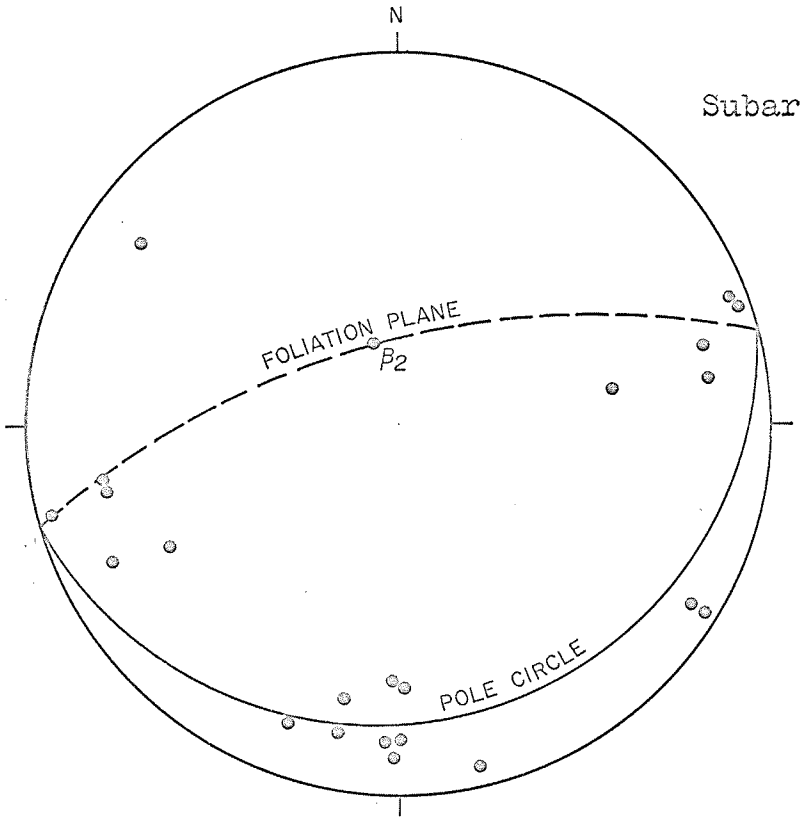

24 poles to bedding.

Plate-8

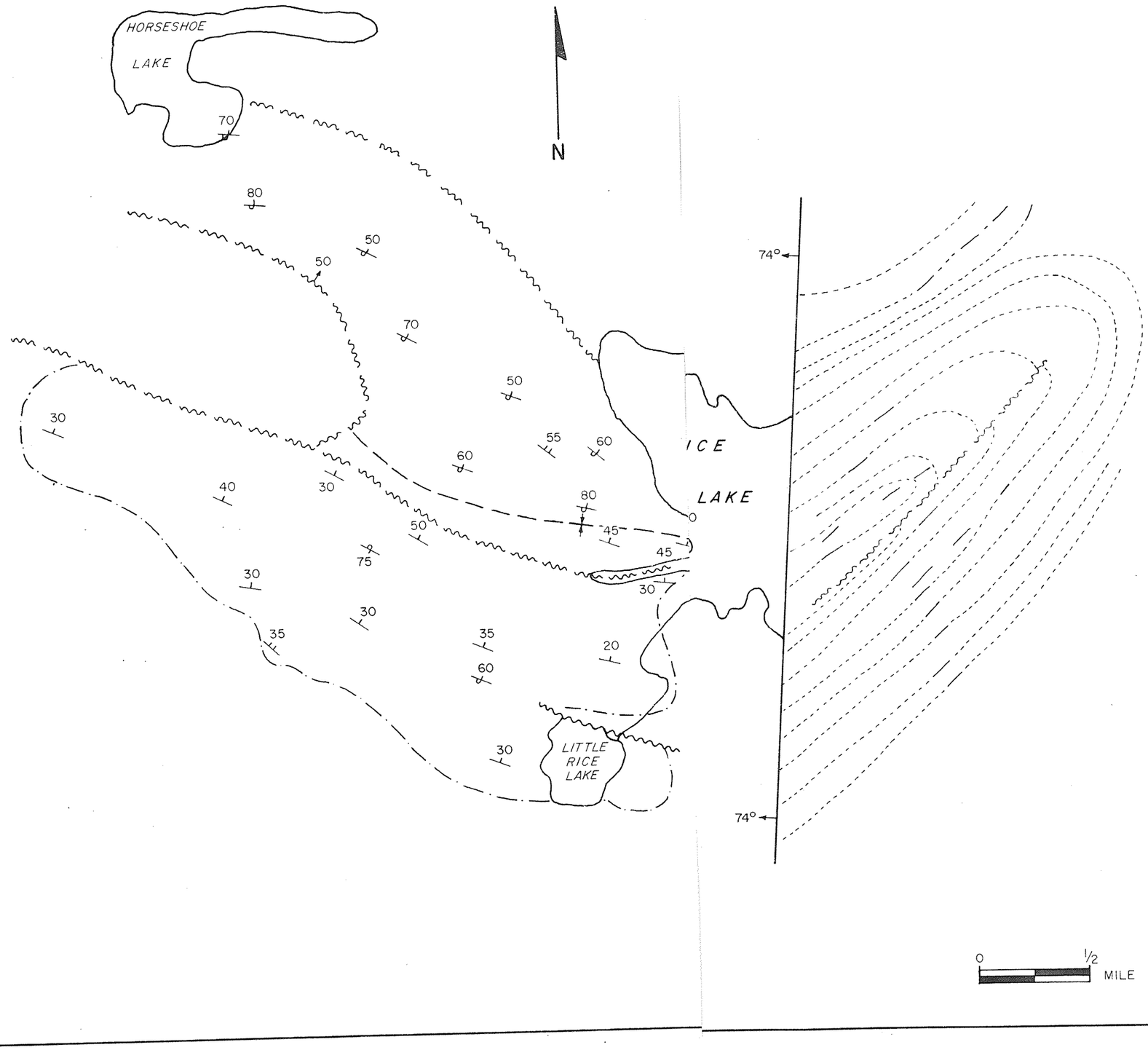

RIGHT SECTION OF THE SAN ANTONIO FORMATION SYNCLINE

PLATE 9

LEGEND

- FAULT
- BEDDING TOP DIRECTION KNOWN
- BEDDING TOP DIRECTION NOT KNOWN
- GEOLOGIC CONTACT
- FORM LINE
- PLANE OF SECTION
- AXIAL TRACE

JUNE 1964

R. J. RECTOR

tion is most strongly developed west and south of Horseshoe Lake. The presence of slickensides on some of the foliation surfaces indicates that this surface is a plane of slip.

Foliation is not readily visible in some of the outcrops of massive quartzite but is revealed by the shear direction in deformed pebbles. In some pebbles the shear direction cannot be identified but the elongation of the pebbles indicate that shearing has taken place. In some instances bedding and foliation are parallel (Plate 10A), but in most places, especially west of Horseshoe Lake, bedding and foliation are at a high angle to one another (Plate 10B). The lineation produced by the intersection of bedding and foliation could not be measured in the field. Stockwell (1938) and Davies (1963) considered this foliation to be axial plane foliation.

A fabric diagram of 21 poles to the foliation from Subarea II is given in Plate 11A. One disperse maximum lying about 20° from the periphery of the net is defined. From this maximum a statistical attitude of the foliation is determined to be N74°E/70°N.

The statistically determined plunge of the anticline "β_2", lies on the foliation plane (Plate 11A). The anticline can be interpreted as a product or modification of slip or shear folding because the foliation plane is a plane of slip and contains "β_2".

Joints

Joints are defined by Billings (1958) as, "divisional planes or surfaces that divide rocks, and along which there has been no visible movement parallel to the plane or surface."

A. Foliation parallel to bedding. Outcrop west of Horseshoe Lake by Bissett highway.

B. Foliation (direction given by pencil) is across the strike of the conglomerate. Outcrop west of Horseshoe Lake.

Plate - 10

A. Subarea II

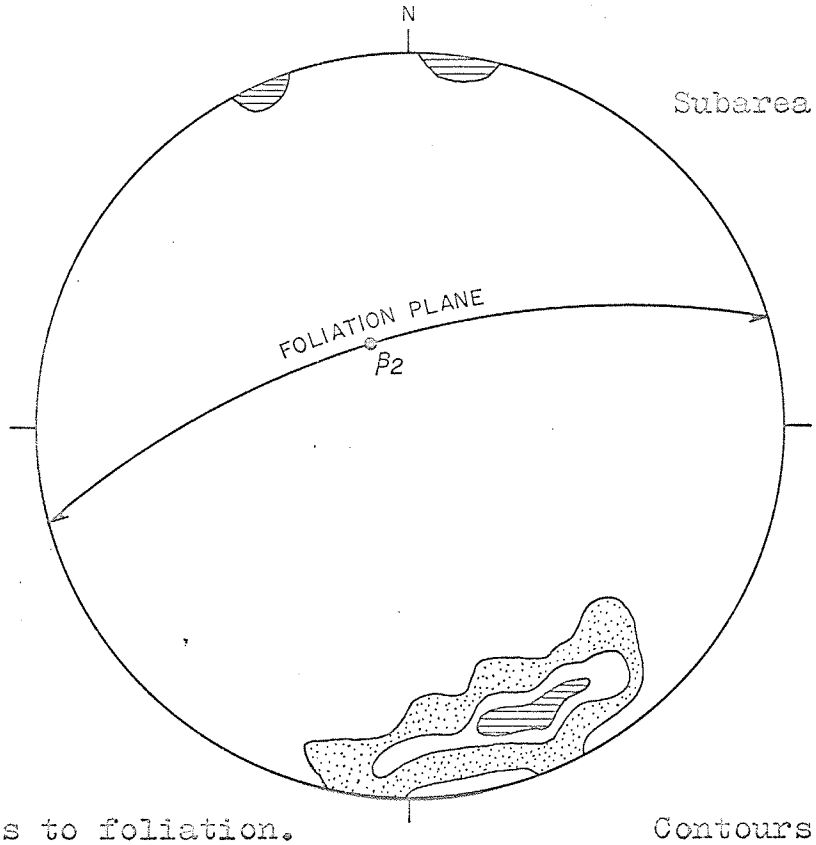

21 poles to foliation.

Contours: 5,15,20%
Max. 28.6%

B.

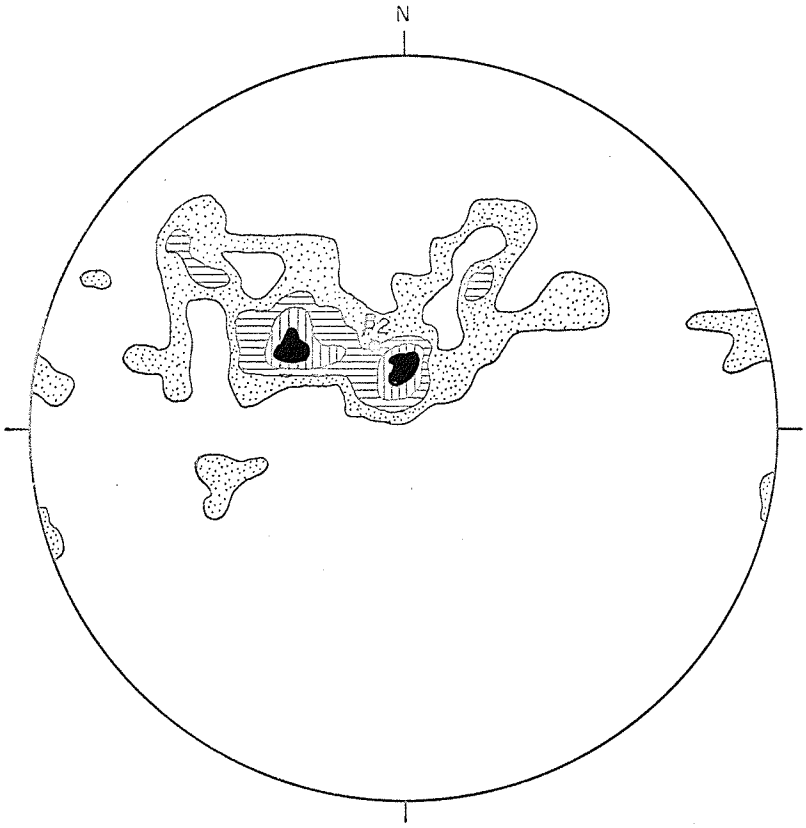

Intersection of bedding and foliation.

26 lineations.

Contour Interval
Max. 17%

Plate-11

Jointing in the San Antonio formation is moderately well developed in most outcrops; however some outcrops have well developed joint sets (Plate 12A). Some joint surfaces have also acted as surfaces of movement (Plate 12B), but the amount of movement could not be determined. An effort was made in the field to record shallow dipping joints which are not as readily observed as those which dip steeply. A total of 129 joint attitudes were collected in a traverse across the formation (Figure 4).

The fabric diagram produced from a plot of the poles to the joint surfaces (Plate 13A) has a peripheral girdle, but three point maxima form the dominant elements in the pattern. The most prominent maximum lies on the periphery while the other two fall within 20° of the periphery. The joint sets represented by these maxima intersect close to a single point.

To examine the relationship of the joint pattern to the syncline, the synclinal axial plane was rotated 35° to the vertical position, and the joint sets were rotated a similar amount around the same axis (Plate 13B). The rotation of the synclinal axial plane to the vertical position was achieved by a 35° rotation about its strike line. In the rotated position one of the joint sets has an attitude 15° away from the attitude of the synclinal axial plane. The most prominent joint direction is almost vertical and is perpendicular to the synclinal axial plane. The remaining joint direction is also almost vertical and has a strike approximately 45° from the strike of the synclinal axial plane.

On the basis of the relationship of the joint geometry of the synclinal fold, the joint sets were classified as; (1) longitudinal joints with an attitude of N76°W/70°NE, (2) cross joints with an attitude of N18°E/ vertical, and (3) shear joints with an attitude of N62°E/75°NW. These attitudes are original attitudes and not the rotated attitudes of the joint analysis. The intersection of the joint sets close to a single point suggests that the joint sets were established

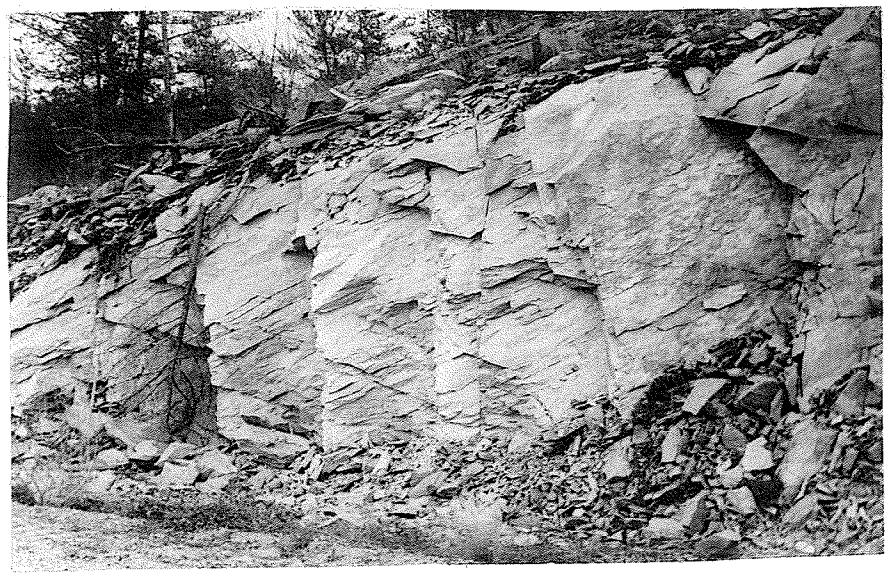

A. Cross joints perpendicular to road bed, shear joints parallel to road bed - San Antonio Formation. Outcrop in roadcut by Horseshoe Lake.

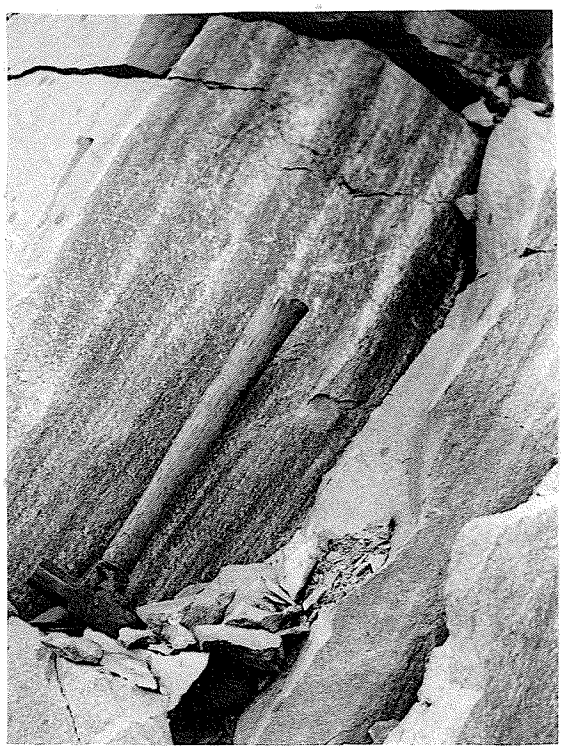

B. Roll structures produced on surfaces of movement. Outcrop in road cut by Horseshoe Lake.

Plate - 12

A.

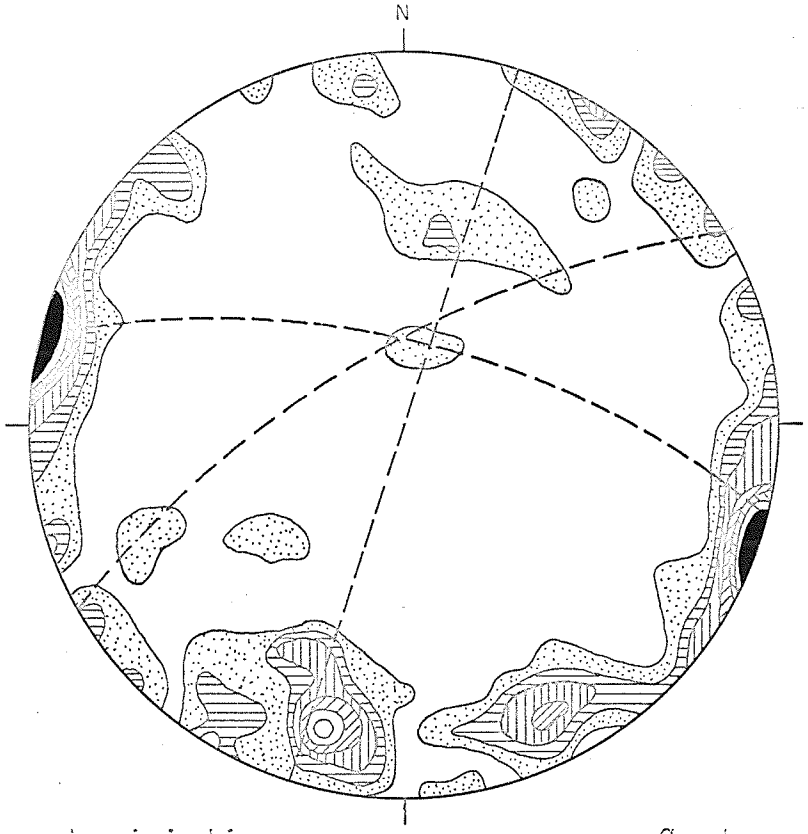

129 poles to jointing.

Contour Interval 1%
Max. 7.5%.

B.

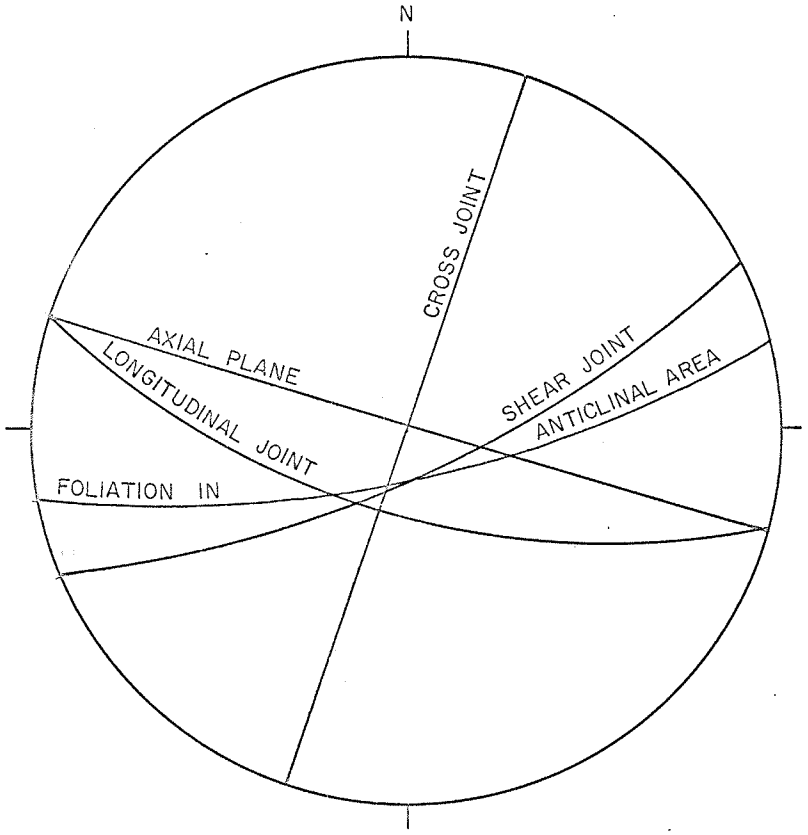

Analysis of Joints
Synclinal Axial Plane Rotated to Vertical

Plate-13

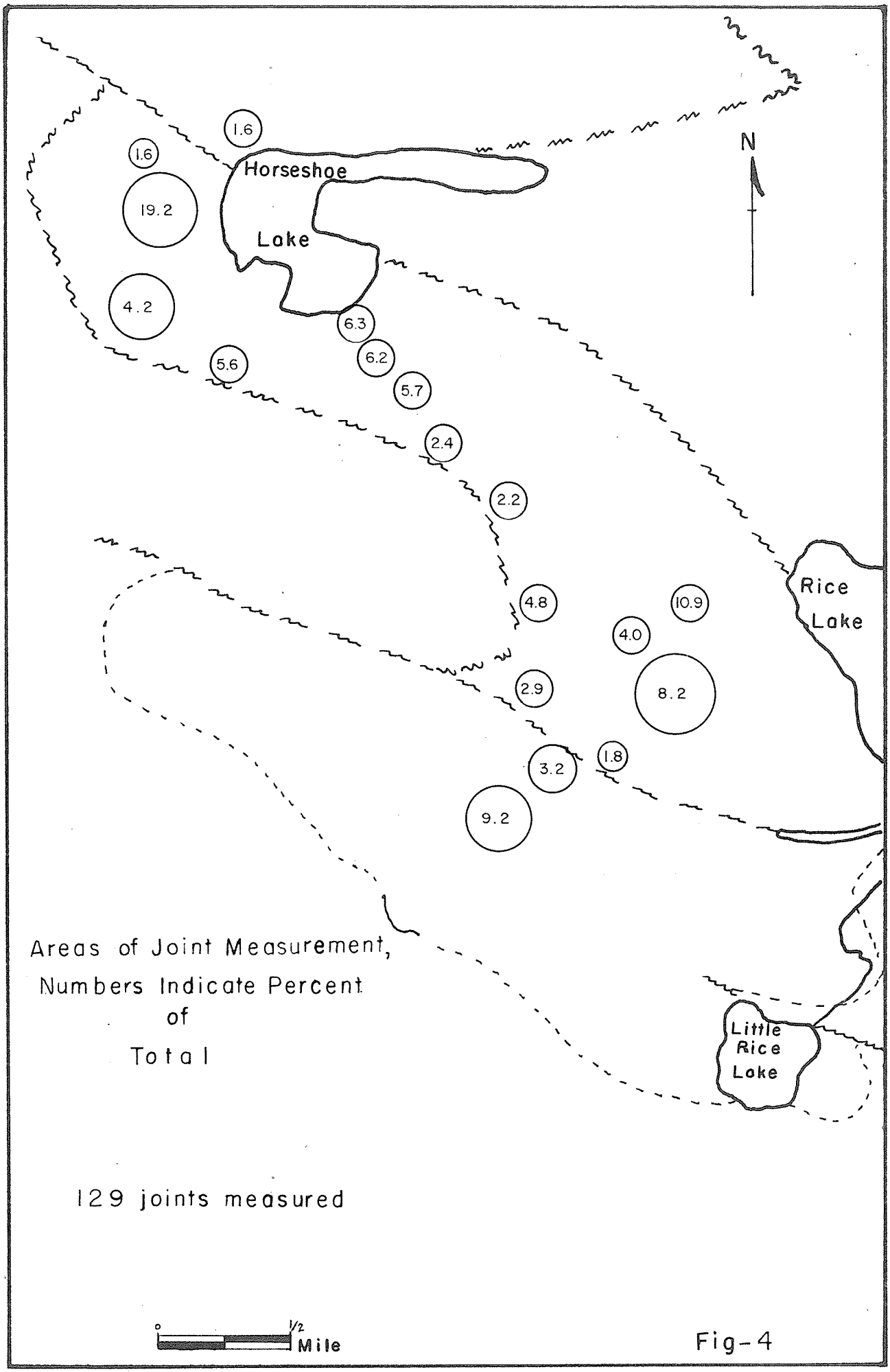
1.6
1.6
19.2
Horseshoe
Lake
4.2
6.3
6.2
5.7
5.6
2.4
2.2
N
Rice
Lake
4.8
10.9
4.0
2.9
8.2
1.8
3.2
9.2
Areas of Joint Measurement,
Numbers Indicate Percent
of
Total
Little
Rice
Lake
129 joints measured
0
1/2
Mile

Fig-4

in the same stress system (Badgley, 1959). The relationship of the joint geometry to the geometry of the syncline would establish the cross joint direction (N18°E/ vertical) as the direction of maximum principal stress (Badgley, 1959).

The joint directions are also valid for the anticlinal fold. The foliation direction in the anticlinal area approximates and is essentially parallel to the shear joint direction (Plate 13B) as defined in the joint analysis of the syncline. On this basis it can be interpreted that the fabric of the anticline was originally similar to that of the syncline, but it would appear that the anticlinal fabric has been modified by a later period of slip folding. The slip folding occurred on slip planes (foliation planes) parallel to the shear direction of the syncline.

Lineations

Cloos (1946) defines lineation as "a descriptive nongenetic term for any kind of linear structure." Lineations in the San Antonio formation are very scarce. The principal types are slickensides, lineations due to the intersection of bedding and foliation, and axes of drag-folds.

Slickensides

The most prominent lineations in the San Antonio formation are slickensides and rolls (Plate 12B) which are developed on surfaces of movement. These surfaces, in most cases, dip steeply and appear to have developed along joint surfaces. Generally, exposures of these surfaces are poor, and only on blasted surfaces were slickensides readily observed.

Analysis of slickensides could not be undertaken due to insufficient data.

Intersection of Bedding and Foliation

The intersection of bedding with foliation forms an important lineation. In the field it was not possible to measure this lineation directly because of the difficulty in observing bedding; the lineation was therefore determined by plotting

both features on a stereographic net.

The fabric diagram of the lineations produced by the intersection of bedding and foliation is given in Plate 11B. Two point maxima which lie on great circles 60° and 75° from the periphery of the net are joined by a dispersed girdle. The fabric diagram is applicable to the area west and slightly south of Horseshoe Lake (approximately equivalent to Subarea II) where the data were obtained.

These maxima can be considered to be one major maximum. This maximum is essentially the same as "β_2", the plunge of the anticline as previously determined.

Other Lineations

Drag-folds, like those north and west of Little Rice Lake, are generally large scale features. Mesoscopic drag-folds (Plate 14A) were observed east of Little Rice Lake in highly sheared and deformed quartzite. The drag-folds in this locality appear to be related to a fault north of Little Rice Lake. The occasional drag-folded quartz vein was observed west of Horseshoe Lake but these appear to be incongruous with the folding of the anticline.

A strong rodding (Plate 15) which forms a prominent lineation in the Rice Lake group was not observed in the San Antonio formation. Although the conglomerate west of Horseshoe Lake is strongly sheared (Plate 14B), the quartzose pebbles and grains have not undergone any apparent rodding. Although pebbles of rhyolite in this conglomerate have been extensively deformed, no prominent rodding was produced.

Synopsis of Mesoscopic Data

The San Antonio formation has been deformed into an anticlinal syn-

A. Drag folds in highly deformed San Antonio Formation. Outcrop east of Little Rice Lake.

B. Differential deformation of pebbles in conglomerate. Outcrop west of Horseshoe Lake.

Plate - 14

Lineation in dacite breccia of the Rice Lake Group.
Outcrop in road cut southeast of Horseshoe Lake.

Plate-15

clinal pair overturned to the south. On the basis of a fabric plot of bedding from the syncline (Subarea I), the syncline plunges 16°/S85°E, whereas the plunge of the anticline ("β_2") is 70°/N15°W (Plate 16A). The plunge of the anticline was determined from a fabric analysis of Subarea II and was found to lie on the foliation plane. The foliation could possibly be axial plane foliation although sufficient bedding information is not available to definitely establish this interpretation. Three well developed joint directions are apparently related to the syncline. The shear joint direction of the syncline is parallel to the foliation in the anticlinal area.

Form of Folding in the San Antonio Formation

An examination of the geologic map and the statistical analysis of the bedding form the basis of delineating the form of folding and the orientation of the external axes of rotation in the San Antonio formation. One major rotational axis (B), (Plate 17) orientated approximately east-west, occurs in the formation. The mesoscopic analysis of the bedding on a stereonet from Subarea I defined the direction of "β_1" (=B) to be 16°/S85°E (Plate 16B). On the basis of this single rotational axis, the syncline was defined as a B tectonite.

Although sufficient field information is not available to define the anticline precisely, a tentative interpretation is proposed. The gross form, the outcrop pattern of a zone of conglomerate, and the bedding west of Horseshoe Lake suggest that the fold plunges to the north-west. Attitudes plotted from the crestal region when plotted on a stereonet indicate a plunge of 70°/N15°W (Plate 16B). On this basis, two additional external axes of rotation (B' $\perp$ B") occur on the anticline (Plate 17). The three mutually perpendicular axes of external rotation classify the anticline as a B$\perp$ B'$\perp$ B" tectonite.

An alternative interpretation can be made of the exterior geometry of

A.

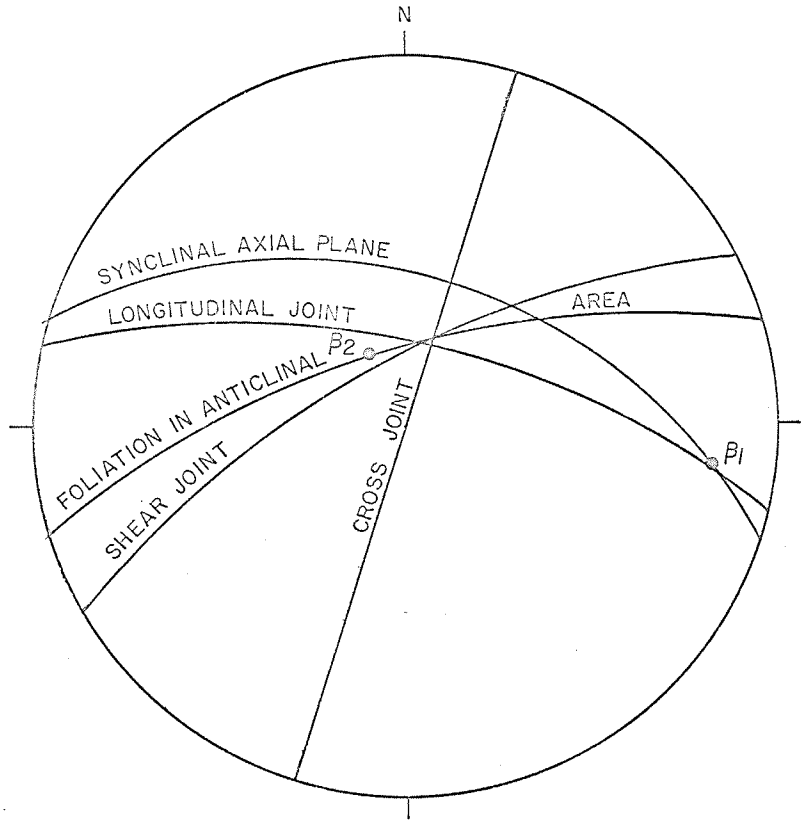

Synopsis of Mesoscopic Data

B.

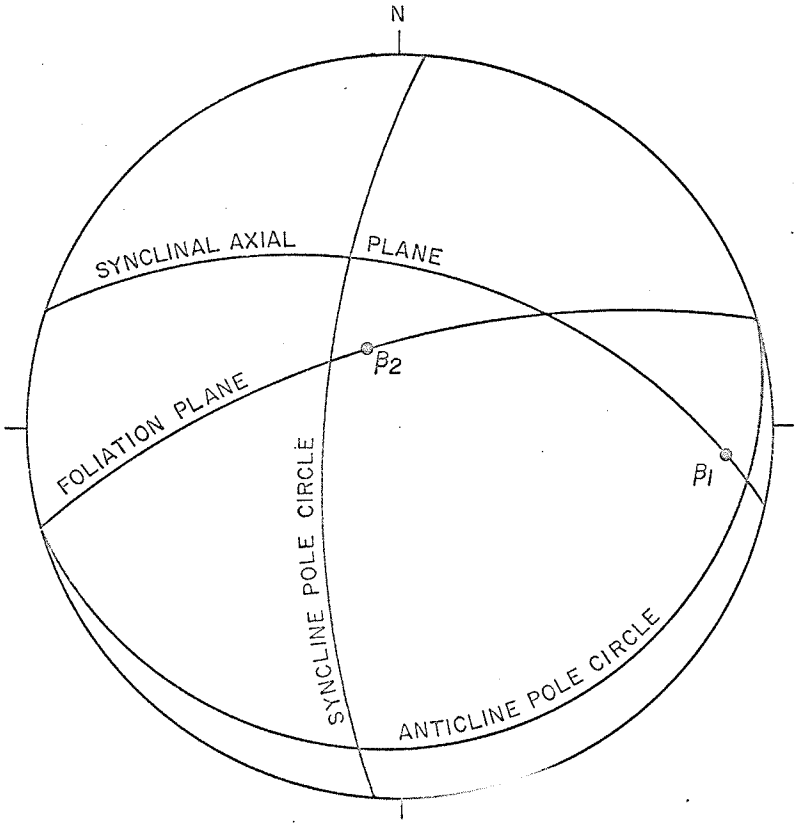

Structural Elements of Folding

Plate-16

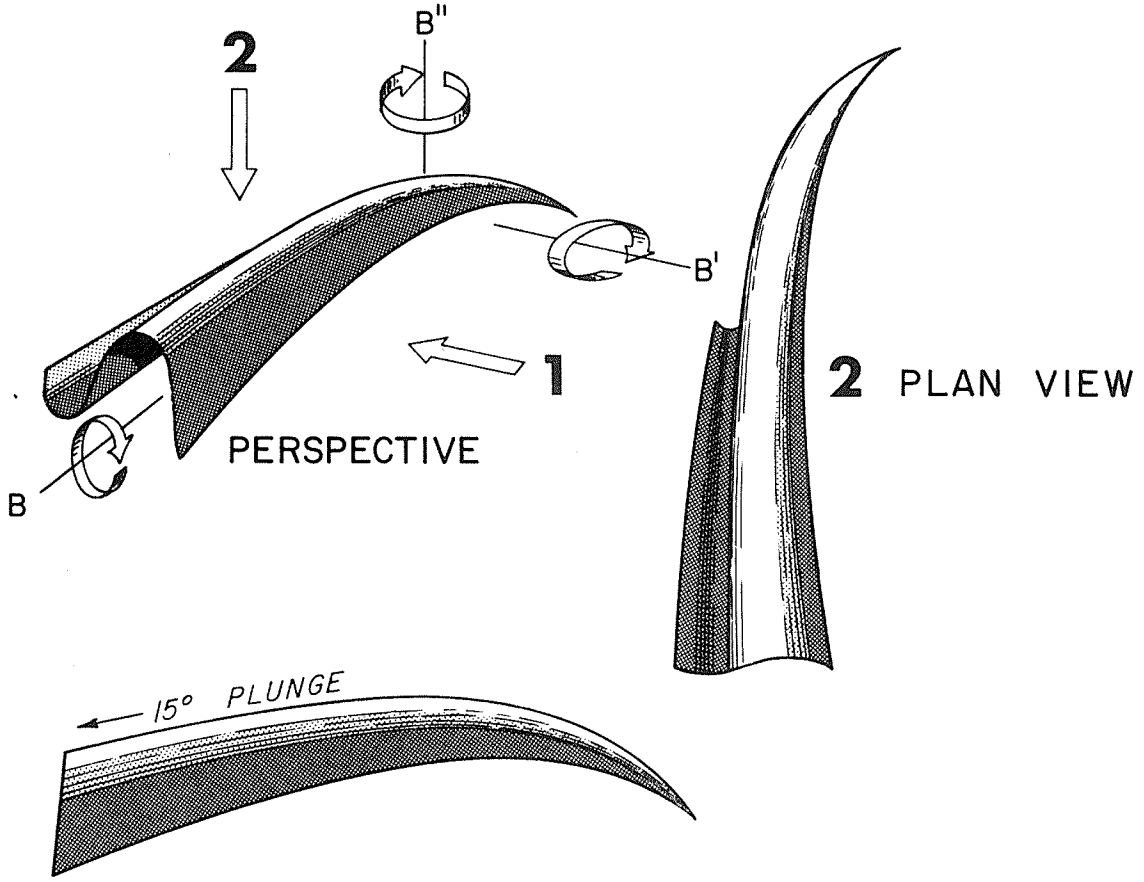

IDEALIZED SKETCH OF FOLDING IN SAN ANTONIO FORMATION WITH THREE AXES OF EXTERNAL ROTATION

PLATE 17

the anticline based on kinematic evidence on the assumption that the anticline was similar to the syncline after flexural slip folding about the "β_1" (=B) axis. The present external geometry can be interpreted as a derived modification caused by differential slip folding. This interpretation is favored because the foliation plane is in fact a slip surface which contains "β_2"; that is the anticline is a product of flexural slip folding and slip folding. On this basis the anticline would be classified as a BΔB' tectonite.

CHAPTER 4

QUARTZ ORIENTATION IN THE SAN ANTONIO FORMATION

General Statement

Sampling Procedure

The sites for collecting samples were chosen using Davies' map (1963). Sampling procedure was such that the main emphasis was placed on the crestal regions of the folds where the most rapid changes in the structural elements were to be expected. Samples on the limbs of the folds were chosen so that a representative suite of specimens across the fold would be obtained. No samples were collected on recognizable shear zones where the fabric produced by folding may have been obliterated. The exact locations of samples are given in Figure 5.

Orientation of samples was achieved by marking on the specimens; (1) a north arrow, (2) a horizontal plane, and (3) the "up" direction.

Laboratory Work

A series of thin sections were cut from the orientated specimens collected in the field. The orientations of c-axes of quartz grains were determined on a 3-axis Cooke universal stage mounted on a Cooke binocular microscope. At least 150 grains were measured for each thin section. All grains were plotted on a Schmidt net, and quartz fabric diagrams were produced by the conventional manner (Knopf, Ingerson, (1938); Turner and Weiss, (1963)). All diagrams were rotated 180° to account for the transposed field of view in a petrologic microscope.

The orientation of quartz c-axes was statistically analyzed in 36 thin sections cut perpendicular to the statistical plunge of the synclinal fold. All the quartz diagrams are drawn such that the center of the net is "β_1" (the plunge of the syncline). The "c^+-c^-" axis on the fabric diagrams is defined as a geometric

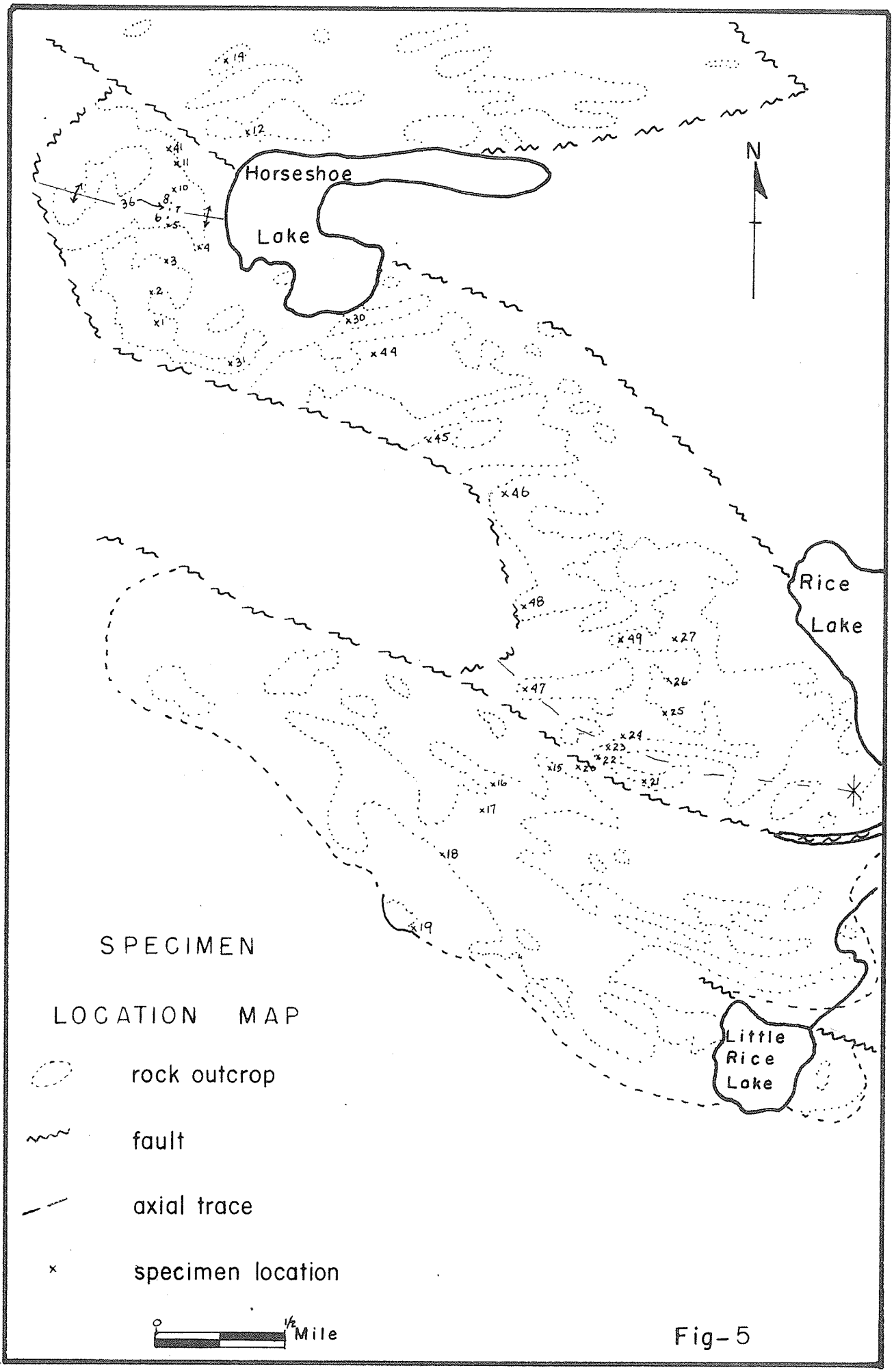
Horseshoe
Lake
N
Rice
Lake
Little
Rice
Lake
SPECIMEN
LOCATION MAP
rock outcrop
fault
axial trace
specimen location
1/2 Mile

Fig-5

axis ("c") and is chosen such that it lies in a vertical plane containing "$\mathcal{B}_1$", and is 90° from "$\mathcal{B}_1$". In similar manner, the "a^+-a^-" axis of the fabric diagrams is a geometric axis ("a") which is perpendicular to the "$\mathcal{B}_1$" and "c" axes. The "a" and the "c" axes are arbitrary geometric axes and are not axes of tectonic transport.

At some localities thin sections were also cut parallel to the "$\mathcal{B}_1$" axis. The fabric from these sections was rotated 90° and compared with the fabric obtained from thin sections cut perpendicular to "$\mathcal{B}_1$". The comparison indicated that the fabric from thin sections cut perpendicular to "$\mathcal{B}_1$" represented true statistical plots of the "c" orientation of quartz, and that the results were not biased by the orientation of the thin section.

The petrofabric diagrams for each specimen are given in the Appendix, Plates 21-38.

Description of Quartz Orientation

General Statement

The orientation of quartz has received more attention than the orientation of any other mineral in tectonites. Orientation of quartz occurs in a variety of ways in different rocks, but particular patterns tend to recur. Although the orientation of quartz has undergone considerable study, the mechanics of quartz orientation are not fully known. Most quartz orientation theories are based on deformation in close relationship to the crystallographic directions in the quartz.

The quartz grains in the red beds of the San Antonio formation embody different deformational characteristics than those in the argillaceous beds, so the orientation patterns of the two types of beds are discussed under separate headings.

Quartz Orientation in the Individual Diagrams

The quartz orientation diagrams are quite variable in detail, but some prominent features recur throughout the series of diagrams. Preferred orientation of quartz c-axes from any particular diagram is usually weak and found to be in the order of 3% to 5%. It is difficult therefore to appraise each diagram separately; thus, a generalized description is given below using as examples the diagrams for RR-15 and RR-19.

Major maxima usually occur in a plane containing "$\mathcal{B}_1$" which is 45° from "a" or "c" (Plate 18). In some diagrams a particular maximum or several maxima may be poorly developed or missing (Plate 18B). A weak or partially developed girdle passing close to the center of the net occasionally joins the maxima (Plate 18A). The maxima usually fall on a small circle approximately 70° from "$\mathcal{B}_1$" (Plate 18) or in the center of the net. The small circle girdle is often distinctly broken close to "a" or "c".

Quartz Orientation in the Argillaceous Beds

The fabric diagram showing the orientation of all measured quartz grains for the argillaceous is characterized by dispersed maxima lying close to the "a-c" plane. The maxima lie on planes containing "$\mathcal{B}_1$" which are 45° from "a" and "c" (Plate 19A). All of these maxima also lie on a small circle girdle, 68° from "$\mathcal{B}_1$", that is distinctly broken at "a". A small maximum occurs at the center of the net at "$\mathcal{B}_1$".

The orientation pattern can be classified as a Maximum IV pattern (Fairbairn, 1949). The microfabric exhibits an orthorhombic symmetry.

Quartz Orientation in the Red Beds

The orientation of the quartz c-axes (Plate 19B) from the red beds

A.

RR.-I5

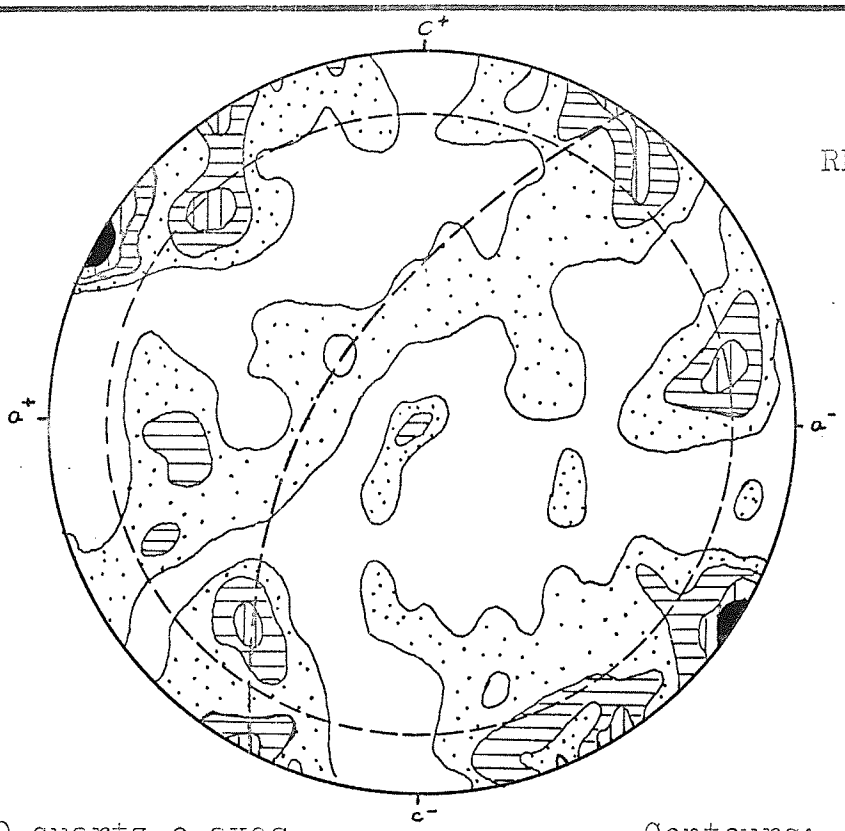

200 quartz c-axes

Contours: .75,I.75, 2.5,3.5 %.

Max. 4%.

B.

RR.-I9

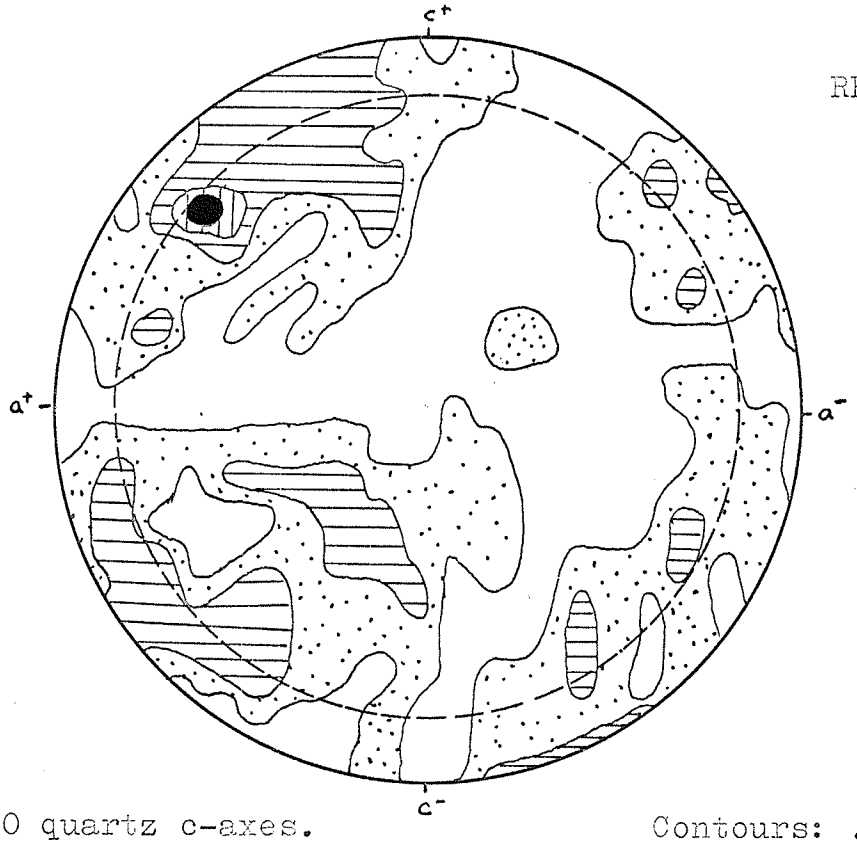

200 quartz c-axes.

Contours: .75,I.75, 2.75,3.75%.

Plate-18

A.

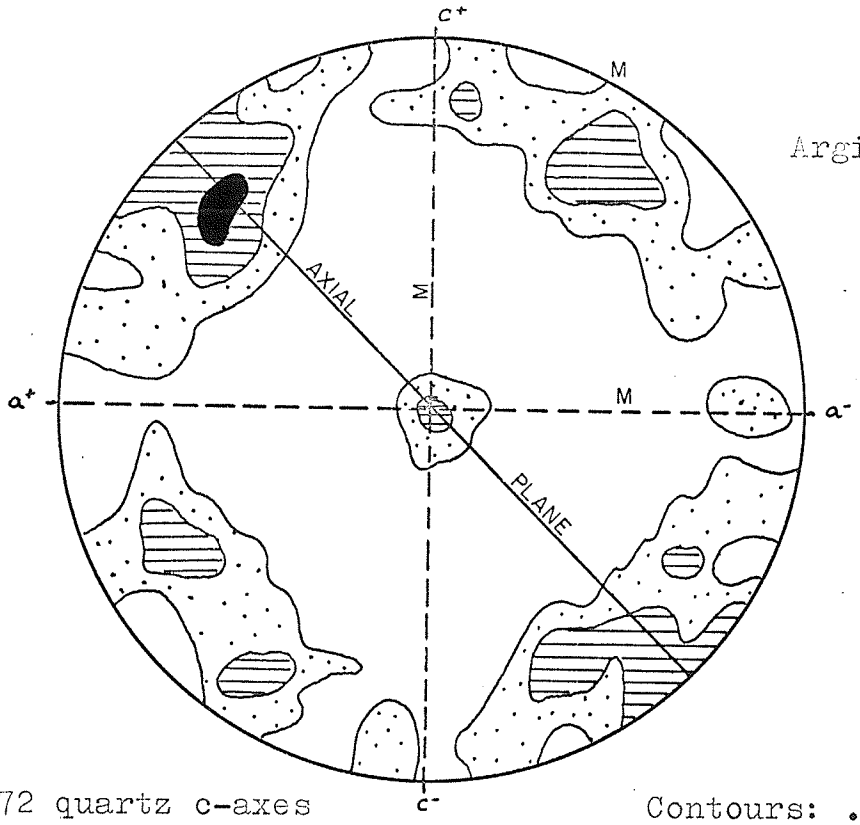

Argillaceous Beds

2372 quartz c-axes

Contours: .9, I.25. 2%.

Max. 2.I%.

M = MIRROR PLANE

B.

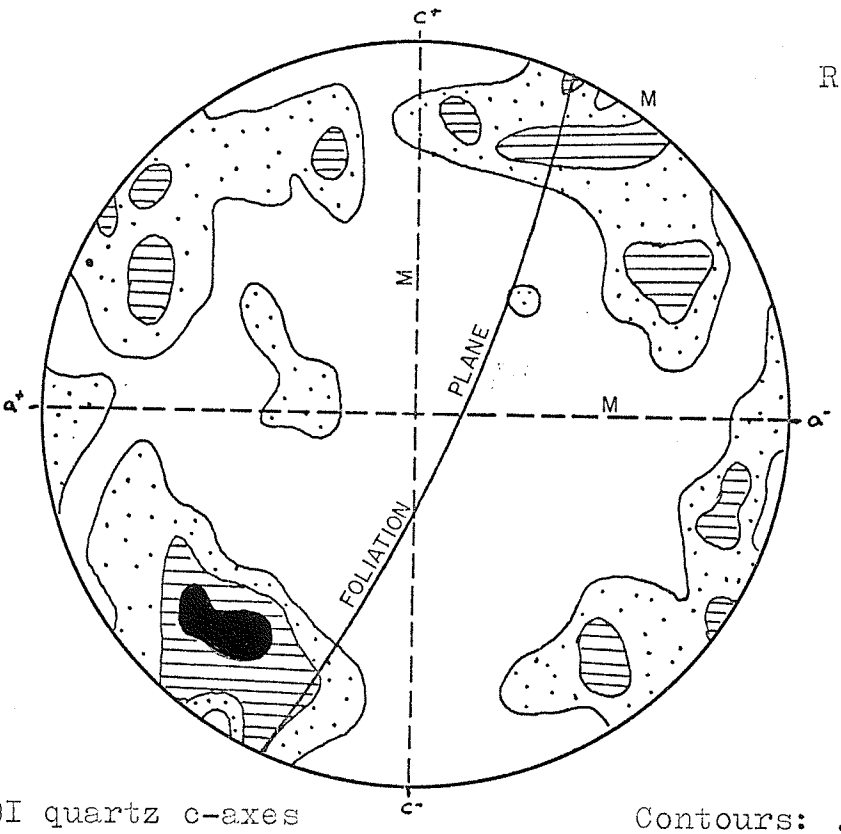

Red Beds

329I quartz c-axes

Contours: .9, I.25, I.45%.

Max. I.6%.

Plate-19

is very similar to the pattern obtained from the argillaceous beds. Four dispersed maxima, lying in two mutually perpendicular planes which contain "$\mathcal{B}_1$" and which are approximately 45° from "a" and "c", characterize the diagram. The maxima also lie on a small circle girdle 68° from "$\mathcal{B}_1$". The small circle girdle is strongly disrupted at "c". The maximum which occurred at "$\mathcal{B}_1$" in the argillaceous beds does not appear in the red beds.

The quartz c-axes have a Maximum IV orientation pattern (Fairbairn, 1949). The orientation pattern of the quartz microfabric in the red beds has orthorhombic symmetry.

Interpretation of the Quartz Orientation

General Statement

An interpretation of the quartz orientation in the folded San Antonio formation was attempted in two ways: (1) an examination of individual petrofabric diagrams for various locations on the fold, and (2) an examination of the synoptic diagrams for the argillaceous beds and for the red beds.

Interpretation of Individual Petrofabric Diagrams

The petrofabric diagrams for the various locations on the folded San Antonio formation are found in the Appendix. An interpretation of the quartz orientation in the individual petrofabric diagrams was attempted by drawing lines from the major and secondary maxima to the center of the net. The line joining the maxima to the center of the net has been termed the q-Richtungen by Ladurner (1954). The bedding was then rotated such that the fold was completely unfolded. During the unfolding the q-Richtungen was rotated with the bedding. The procedural methods for unfolding a fold and the rotation of q-Richtungen with the bedding are described by Jones (1959), and Ball (1960).

Ideally, in the case of a rotational fold, when the bedding is unfolded the q-Richtungen from all locations on the fold would assume a parallel alignment providing the quartz c-axes were aligned before folding (Ball, 1960). In the case of the petrofabric diagrams from the San Antonio formation, the q-Richtungen did not assume a parallel orientation when the fold was unfolded.

Assuming that the statistical concentrations are real, the non-parallel alignment of the q-Richtungen after unfolding may be attributed to any one of a number of factors suggested below.

(1) The fold has not been properly unfolded if a single pre-deformational orientation of quartz c-axes existed. This may be due to the fact that the exact form of the fold is not known to the degree of precision required to carry out the unfolding.

(2) A more complex pre-deformational fabric with more than one preferred orientation of quartz c-axes existed; or a variable orientation of c-axes from plane to plane was present. In this case the unfolding of the fold would not make the c-axes parallel.

(3) The quartz fabric is not a simple rotational fabric. The fabric may instead be the result of recrystallization under stress or any combination of rotation and recrystallization.

With the information available, it was not possible to appraise the effects of the factors which may have contributed to the non-parallel alignment of the q-Richtungen.

Interpretation of the Synoptic Petrofabric Diagrams

General Statement

Two synoptic diagrams were prepared, one for the argillaceous beds, and the other, for the red beds (Plate 19).

The diagram for the argillaceous beds approximately covers the areal extent of the syncline, and the diagram for the red beds approximates the extent

of the anticlinal fold. This subdivision also groups the two distinct types of quartz grains found in the San Antonio formation: the large undulose grains in the red beds and the recrystallized grains in the argillaceous beds.

The petrofabric diagrams for the argillaceous beds and the red beds are very similar, and are characterized by two major elements. Four maxima lie in two mutually perpendicular planes which are 45° from "a" and "c" and contain "$\mathcal{B}_1$". The maxima also lie on a 70° small circle girdle the center of which is "$\mathcal{B}_1$".

An interpretation of the synoptic diagrams involves not only a study of the diagrams themselves but also a study of the diagrams in conjunction with the form of the fold. The following interpretations of the orientation patterns of the quartz c-axes are considered.

(1) The orientation pattern represents rotation about a fold axis.

(2) The orientation pattern is due to recrystallization in a stress field.

Rotational Fabric

The maxima in both the argillaceous and the red beds fall on a small circle approximately 70° from "$\mathcal{B}_1$", and lie on two mutually perpendicular planes which contain "$\mathcal{B}_1$" and are 45° from "a" and "c". This orientation pattern has been cited by previous workers as evidence of a rotational fabric (Fairbairn 1939, Turner 1948). A rotational fabric is one in which a single preferred orientation of quartz c-axes has been rotated to give the observed orientation pattern. On this basis, the San Antonio formation could be classified as a B tectonite. Turner (1948) defines a B tectonite as follows:

> "b (=B) axis of the fabric... and at the same time the axis of external rotation about which s surfaces have been folded by flexure, and individual grains or aggregates of grains bodily rotated with or without internal deformation."

However, folding in the San Antonio formation is overturned and almost isoclinal, which virtually means 180° rotation, that is the fabric has been inverted and that the pre-folding fabric would have had the presently observed pattern.

A dispersed small circle girdle can be produced by rotation of single quartz c-axes concentration about "β_1". The observed orientation pattern could only be achieved if the "β_1" axis is 70° to the pre-existing alignment of quartz c-axes. The tendency toward development of a small circle girdle is distinctly disrupted at "a" in the argillaceous beds, and at "c" in the red beds. Of these two factors only the disruption of the small circle girdle at "a" or "c" tends to oppose the interpretation that the observed fabric is due to rotation.

In view of the fact that the folding is almost isoclinal, only one pair of maxima would be expected to occur in the petrofabric diagrams if the pre-deformational fabric had a single concentration. However, if two pre-deformational concentrations existed then the observed microfabric would be possible.

Fabric due to Compressive Stress

The orientation of the quartz microfabric of the San Antonio formation is such that the maxima may be considered to lie in the conjugate planes of maximum shear stress development, if the orientation of "β_1" is assumed to be in the same orientation as the intermediate principal stress.

Experimental work by Griggs (1960) established that the syntectonic recrystallization of quartz during shearing was such that the quartz axes lie on the shear plane and on a plane normal to the shear.

Experimental work by Borg et al (1960) on the St. Peter sandstone produced orientation patterns similar to those of the San Antonio formation.

Plate 20 illustrates the orientation patterns obtained from the St. Peter sandstone under stress conditions in which $\sigma_2 = \sigma_3$. The pattern is not identical to that of the San Antonio quartzite because of differing stress conditions, however a similarity exists between the deformed San Antonio formation and the experimentally deformed St. Peter sandstone.

Syntectonic recrystallization can account for the orientation mechanism in the argillaceous beds; however, there is very little evidence of recrystallization of the quartz in the red beds. Orientation of quartz may be achieved by crystal gliding on the (0001) translation plane. Boehm lamellae and deformation bands parallel to the (0001) have been cited as visual evidence of translation on (0001) of quartz (Hietanen, 1938). Boehm lamellae are rare in the San Antonio formation and a statistical study of the undulatory bands in the quartz grains of the red beds was not undertaken. Crystal gliding parallel to (0001) may provide an orientation mechanism for quartz in the red beds of the San Antonio formation.

Regardless of the orientation mechanism of the quartz c-axes, the essential element is the symmetry of the quartz fabric. The quartz microfabric of the San Antonio formation is orthorhombic but is heterotactic with respect to the axial plane of the syncline and the foliation plane in the anticlinal area as determined by mesoscopic analysis (Plate 19). The two mutually perpendicular planes containing the quartz c-axes maxima are not symmetry planes because the small circle girdle is disrupted at "a" in the argillaceous beds and at "c" in the red beds. A heterotactic relationship exists between the microfabric and the mesoscopic fabric because the mesoscopic elements (the axial plane of the syncline and the foliation plane of the anticlinal area) are not contained by the symmetry planes of the quartz microfabric. This relationship indicates that the mesoscopic and the microscopic fabrics cannot be explained by the same stress system. If the

A.

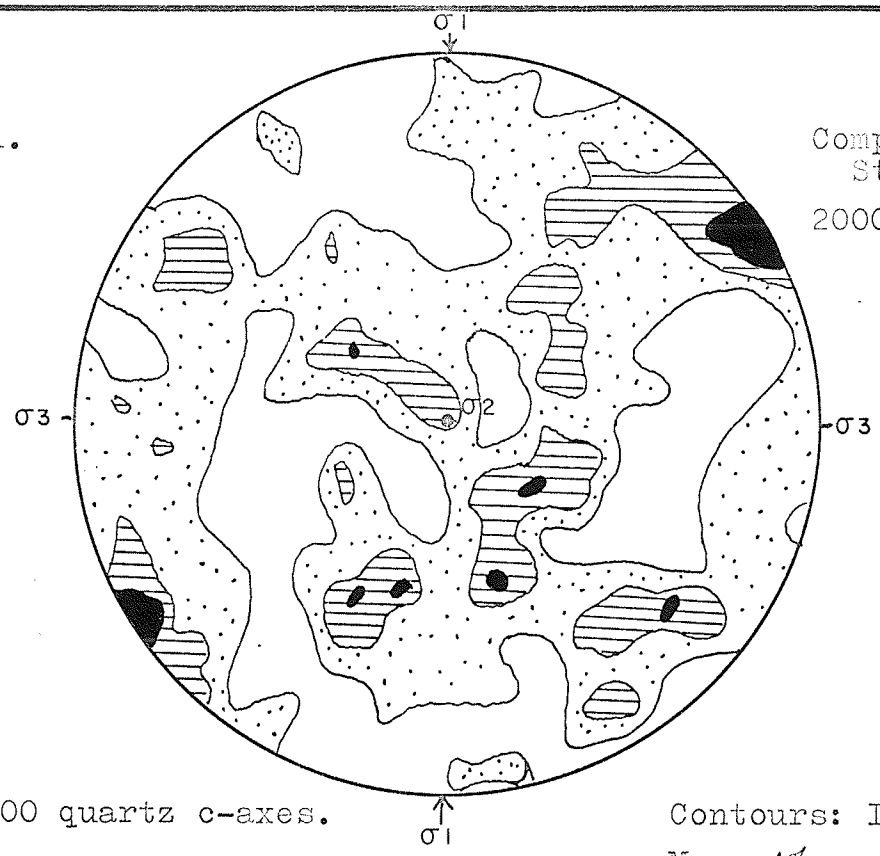

Compressive Stress 2000 bars.

200 quartz c-axes.

Contours: I, 2, 3%.
Max. 4%.

$\sigma 2 = \sigma 3$

B.

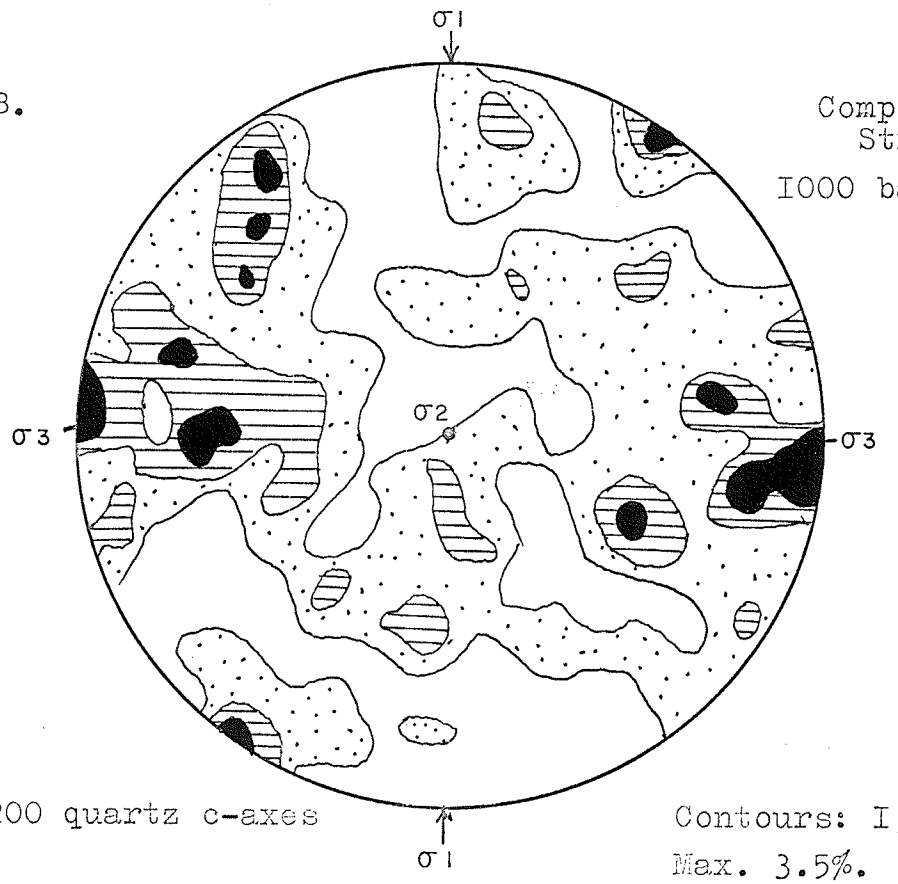

Compressive Stress I000 bars.

200 quartz c-axes

Contours: I, 2, 3%.
Max. 3.5%.

Plate-20 (after Borg et al (I960))

quartz fabric is the result of a separate system, it appears likely that it would have postdated the stresses producing the folding.

The orthorhombic symmetry of the quartz fabric can be correlated to the local stress system in which it was formed and its initial fabric (Turner and Weiss, 1963). Although the initial fabric of the San Antonio formation is unknown, the symmetry of the stress system can be the same or a higher order than that of the quartz microfabric (Turner and Weiss, 1963). The stress system and the preferred orientation of the quartz are likely to have some symmetry elements in common.

The three mutually perpendicular symmetry planes can be assumed to contain the three axes of principal stress. On this basis, the orientation of the intermediate principal stress direction (σ_2) may be defined by "β_1", therefore either the "a" or "c" geometric axes could be the axis of maximum principal stress, because both lie 45° from the S planes in which the quartz maxima lie. In the view of the fact that the macroscopic elements (direction of overturning and the interpreted direction of thrusting), and the mesoscopic elements (joints) indicate a compressive stress from the north, the "a" geometric axis may be interpreted as the direction of maximum principal stress, σ_1, and "c" becomes the direction of the minimum principal stress σ_3. Orientation of the stress axes are:

(1) maximum principal stress direction, 0°/N6°E,

(2) intermediate principal stress direction, 16°/S85°E,

(3) minimum principal stress direction, 74°/N84°W.

In summary, the following points can be made from an interpretation of the microfabric:

(1) The orientation pattern throughout the formation is essentially similar.

(2) The microfabric in the argillaceous beds does not appear to be rotational and is better explained by recrystallization in a stress field as a result of

compressive stress.

(3) The microfabric in the red beds also does not appear to be rotational but may be explained as the result of translation gliding along the (0001) crystallographic plane of quartz although conclusive evidence is not available in the San Antonio formation.

(4) Although the quartz grains in the red beds have different deformational characteristics than the quartz grains in the argillaceous beds, it appears that the same stress or stresses caused orientation in both members.

(5) It would appear that the well developed foliation in the red beds did not have an effect on the orientation of the quartz axes because the orientation pattern is similar in both members of the formation.

(6) No evidence could be found in the quartz fabric of the San Antonio formation to suggest a primary fabric. In outward appearance the microfabric resembles the fabric described by Higgins (1947) and Turner (1940). In these cases and in the San Antonio formation the fabric appears to have had some relationship to the stress ellipsoid.

Discussion of Stresses Responsible for Deformation and Orientation of Quartz

The quartz grains of the San Antonio formation are of two types: the undulose grains of the red beds and the recrystallized grains of the argillaceous beds. These two types of deformation can be interpreted as:

(1) a response to different deformational stresses,

(2) a different response to the same stress by the quartz grains in each member, that is recrystallization in the argillaceous beds and possible translation gliding in the red beds.

The preferred orientation of the quartz c-axes is consistent throughout

the formation; therefore the second interpretation is favored. The orientation of the quartz in the argillaceous beds appears due to syntectonic recrystallization, whereas, crystal gliding parallel to (0001) may possibly be the orientation mechanism in the red beds.

An explanation for the different behavior of the quartz grains to the same stresses may be attributed to compositional differences. In the argillaceous beds, some of the stresses could be taken up by slip on the argillaceous films in the quartzite. The same stress acting on the red beds could not be relieved by slip because of the scarcity of argillaceous material. This effect may have produced the highly strained quartz and fractured feldspar in the red beds.

The quartz microfabric is similar throughout the formation and is heterotactic with respect to the axial planes of the folded San Antonio formation (Plate 19). The heterotactic relationship of the microfabric and the mesoscopic fabric, and the similar c-axes orientation throughout the formation suggests that the microfabric was impressed late in the structural development of the San Antonio formation. Nevertheless a relationship does exist between the microfabric and macrofabric. The direction of maximum principal stress σ_1, as determined by the microfabric indicates a 0°/N6°E orientated stress. This is in agreement with the direction of overturning and thrusting (Davies, 1963) as indicated by the macrofabric. Slight dispersion of the quartz maxima suggests that, although the orientation of the quartz is due to a compressive stress, a slight amount of rotation may have occured after the initial development of the quartz orientation.

In summation, quartz orientation in the red beds and the argillaceous beds was produced by the same stress or stresses. The orientaning stress is believed to be a north south compressive stress acting in a horizontal plane.

SUMMARY AND CONCLUSIONS

The macroscopic, mesoscopic and microscopic fabric elements of the San Antonio formation were analyzed in order to interpret the evolution of the structure within the San Antonio formation.

On the basis of a mesoscopic analysis of the bedding; the syncline plunges 16°/S85°E whereas the anticline plunges 70°/N15°W, and the fold axis of the anticline ("B_2") lies on the foliation plane. Three well developed joint directions are apparently related to the syncline. The relationship of the joint geometry to the geometry of the syncline established the cross joint direction (N18°E/vertical) as the direction of maximum principal stress.

The foliation in the anticlinal area was identified as a plane of slip that is approximately parallel to the shear joint direction as defined by the joint analysis of the syncline. On this basis, the anticline was interpreted to be a modification by a later period of slip folding of a fabric that essentially may have been similar to that of the syncline. The shear folding occurred on slip planes (foliation planes) parallel to the shear joint direction.

An analysis of the c-axes orientation of the quartz grains established similar petrofabric diagrams for both the argillaceous beds and the red beds. The diagrams are characterized by four dispersed maxima lying close to the "a-c" plane. The maxima lie on two mutually perpendicular planes which contain "B_1", and are approximately 45° from "a" and "c". All the maxima lie on a small circle girdle, 68° from "B_1" that is distinctly broken at "a" in the argillaceous beds and at "c" in the red beds. The microfabric symmetry is orthorhombic but is heterotactic with respect to the axial plane of the syncline and the foliation plane of the anticlinal area.

No evidence could be found in the quartz fabric to suggest a primary

fabric but the microfabric appears to have had some relationship to the stress ellipsoid. The quartz microfabric does not appear to be rotational but is better explained by recrystallization in a stress field in the argillaceous beds and possibly crystal gliding parallel to the (0001) of quartz in the red beds as a result of a compressive stress. The orientation of the maximum principal stress direction from the quartz microfabric was determined to be 0°/N6°E.

Although sufficient information is not available to precisely define the folding in the San Antonio formation, all the fabric elements (macroscopic, mesoscopic and microscopic) indicate that the deformation was caused by a north south orientated compressive stress acting in a horizontal plane.

BIBLIOGRAPHY

Badgley, P.C., (1959): Structural Methods for the Exploration Geologist; Harper Bros., N.Y.

Ball, T.K., (1960): A Petrofabric Analysis of a Fold; Amer. Journ. Sci., Vol. 258, pp. 274-281.

Billings, M.P., (1958): Structural Geology; 2nd. edition, Prentice Hall, N.J.

Bonham, L.C., (1957): Structural Petrology of the Pico Anticline, Los Angeles County, California; Jour. Sed. Petrology, Vol. 27, no. 3, pp. 453-475.

Borg, I. et al, (1960); Experimental Deformation of St. Peter Sand: A Study of Cataclastic Flow; Rock Deformation; Geol. Soc. Amer. Mem. 79, pp. 133-192.

Cloos, E., (1946): Lineation, A Critical Review and Annotated Bibliography; Geol. Soc. Amer. Mem. 18.

Cooke, H.C., (1921): Geology and Mineral Resources of Rice Lake and Oiseau River Areas, Manitoba; Geol. Surv., Canada, Sum. Rept. 1921, pt. C, pp. 1-35.

Dahlstrom, C.D.A., (1954): Statistical Analysis of Cylindrical Folds; Trans. Can. Inst. of Min. and Metallurgy, Vol. 57, pp. 140-145.

Davies, J.F., (1949): Geology of the Wanipigow Lake Area, Manitoba; Man. Mines Branch prelim. rept. 48-2.

——————— (1950): Geology of the Wanipigow River Area, Manitoba; Man. Mines Branch pub. 49-3.

_____ (1953): Geology and Gold Deposits of the Southern Rice Lake Area, Manitoba; Man. Mines Branch pub. 52-1.

_____ (1963): Geology and Gold Deposits of the Rice Lake - Wanipigow River Area; unpub. Ph. D. Thesis, Univer. of Toronto.

Davies, J.F., et al, (1962): Geology and Mineral Resources of Manitoba; Man. Mines Branch.

Fairbairn, H.W., (1939): Hypothesis of Quartz Orientation in Tectonites; Bull. Geol. Soc. Amer., Vol. 50, pp. 1475-1492.

_____, (1949): Structural Petrology of Deformed Rocks; 2nd edition, Addison-Wesley, Mass.

Griggs, D.T., et al (1960): Deformation of Rocks at 500° to 800°C; -- Rock Deformation; Geol. Soc. Amer. Mem. 79, pp. 133-192.

Hietanen, A., (1938): On the Petrology of the Finnish Quartzites; Helsinki, Government Press.

Higgins, J.W., (1947): Structural Petrology of the Pine Creek Area, Dickinson County, Michigan; Journ. of Geol., Vol. 55, pp. 476-489.

Jones, K.A., (1959A): The Significance of Schnitteffekt in Petrofabric Diagrams; Amer. Journ. Sci., Vol. 257, pp. 55-62.

_____ (1959B): A Petrofabric Method of Fold Analysis; Amer. Journ. Sci. Vol. 257, pp. 138-143.

Knopf, E.B., and Ingerson, E., (1938): Structural Petrology; Geol. Soc. Amer., Mem. 6.

Ladurner, J., (1954): Beitrage zur Typisierung von Quartzfalten; Tschermaks Minerlog. Petrog. Mitt. F. 3, B and 2, pp. 47-66.

Lowdon, J.A., (1961): Age Determinations by the Geological Survey of Canada; Geol. Surv. Canada Paper 61-17, (Rept. -2, Isotopic Ages).

Moore, E.S., (1912): Region East of the South End of Lake Winnipeg; Geol. Surv. Canada, Summ. Rept. 1912, pp. 262-270.

Riley, N.A., (1947): Structural Geology of the Baraboo Quartzite; Jour. Geol., Vol. 55, pp. 453-475.

Sander, B., (1930): Gefugekunde der Gesteine; Vienna, Springer.

Stanton, M.S., (1941): Heavy Accessory Mineral Study Applied to Local Pre-Cambrian Correlation; Unpub. M.A. Thesis, Queens Univ., Kingston.

Stockwell, C.H., (1938): Rice Lake-Gold Lake Area, Southeastern Manitoba; Geol. Surv. Canada, Mem. 210.

_____ (1940): Gold Mines and Prospects in the Rice Lake - Beresford Lake Area, Manitoba; Trans. Can. Inst. Min. and Metal., Vol. 43, pp. 613-626.

_____ (1945): Geological Map 810A, Rice Lake; Geol. Surv. Canada.

Turner, F.J., (1940): Structural Petrology of the Schists of Eastern Otago, New Zealand; Amer. Jour. Sci., Vol. 238, pp. 73-106, 153-191.

_____ (1948): Mineralogical and Structural Evolution of the Metamorphic Rocks; Geol. Soc. Amer., Mem. 30.

Turner, F.J. and Weiss, L.E., (1963): Structural Analysis of Metamorphic Tectonites; McGraw-Hill, N.Y.

Wright, J.F., (1922): Rice Lake Map Area, Southeastern Manitoba; Geol. Surv. Can. Summ. Rept., 1922, pt.C, pp. 45-73.

_____ (1923): Geological Map 1992; Geol. Surv. Can.

_____ (1925): Central Manitoba Gold Field, Some Geological Notes on East Central Manitoba (Rice Lake) Gold Area; Can. Mining Jour., Vol. 46, pp. 91-95,

_____ (1927): Geological Map 195A, Beresford and Rice Lakes Area; Geol. Surv. Can.

_____ (1932): Geology and Mineral Deposits of a Part of Southeastern Manitoba; Geol. Surv. Can., Mem. 169.

APPENDIX

Petrofabric Diagrams Showing Quartz Orientation in the San Antonio Formation

The petrofabric diagrams which follow show the orientation of quartz c-axes for individual specimens. The field locations of specimens are given in Figure 5. The diagrams are presented in a south to north sequence across the formation.

The thin sections are cut perpendicular to the statistical plunge of the synclinal fold "$\mathcal{B}_1$", 16°/S85°E. All the quartz diagrams are drawn such that the center of the net is "$\mathcal{B}_1$". The "c^+-c^-" axis on the fabric diagrams is defined as the geometric axis ("c") and is chosen such that it lies in a vertical plane containing "$\mathcal{B}_1$", and is 90° from "$\mathcal{B}_1$". In similar manner, the "a^+-a^-" axis of the fabric diagrams is a geometric axis "a" which is perpendicular to the "$\mathcal{B}_1$" and the "c" axes. The "a" and the "c" axes are arbitrary geometric axes and are not axes of tectonic transport.

The letter A or B which occurs in the upper left hand corner of the diagrams refers to Figure A or B of that particular plate. The upper right hand corner contains the specimen numbers of the thin sections, and these correspond to the specimen numbers on the location map (Figure 5). The lower left hand corner gives the number of quartz c-axes determined in that particular thin section. The values of the contour lines are given in the lower right hand corner along with the maximum concentration of quartz c-axes per 1% area in the petrofabric diagram.

A.

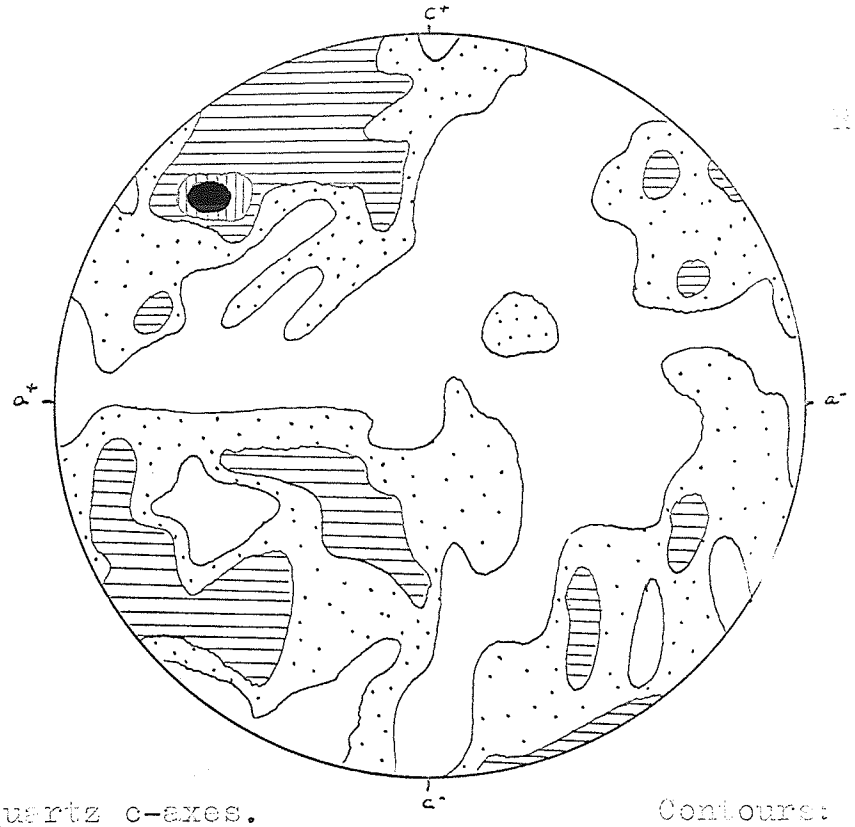

N.R. I9

200 quartz c-axes.

Contours: .75, 1.75, 3.75%.

Max. 4%

B.

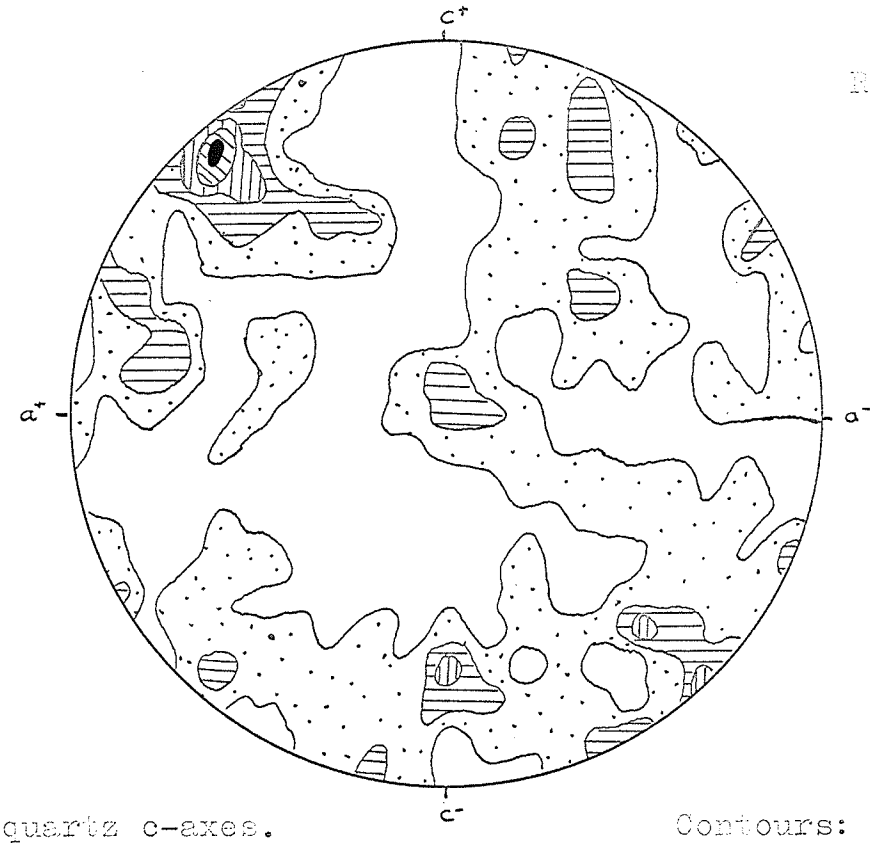

N.R.-I8

200 quartz c-axes.

Contours: .75, 1.75, 3.75, 4.75%.

Max: 5%

Plate-2I

A. R.R.-I7

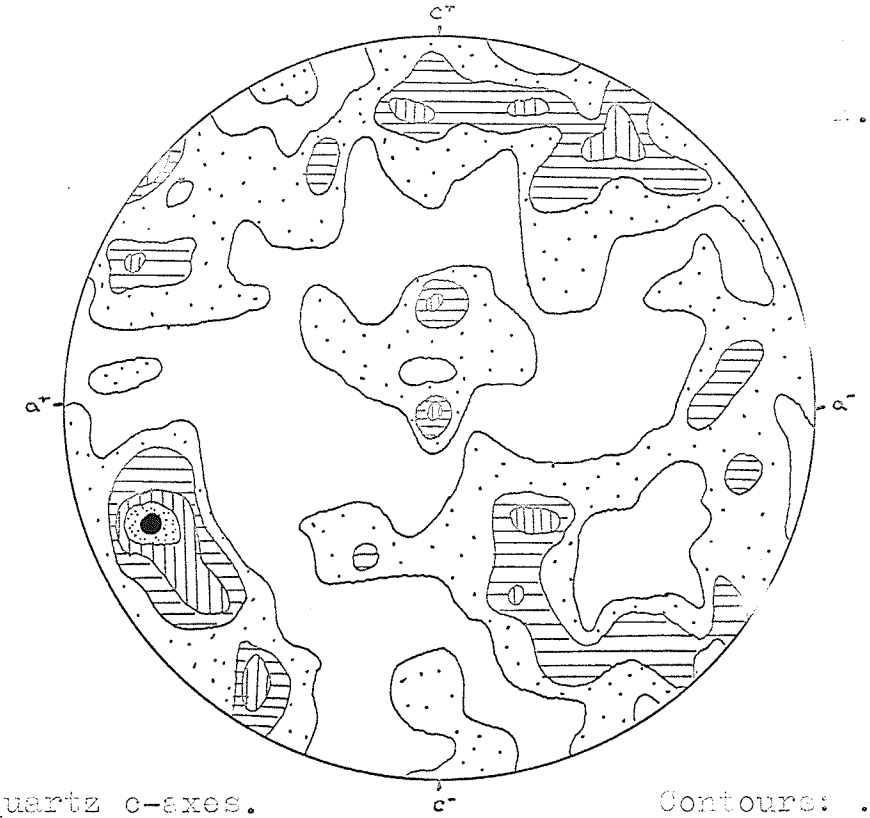

200 quartz c-axes. Contours: .75, I.75, 2.5, 3.5%.

Max. 4%

B. R.R.-I6

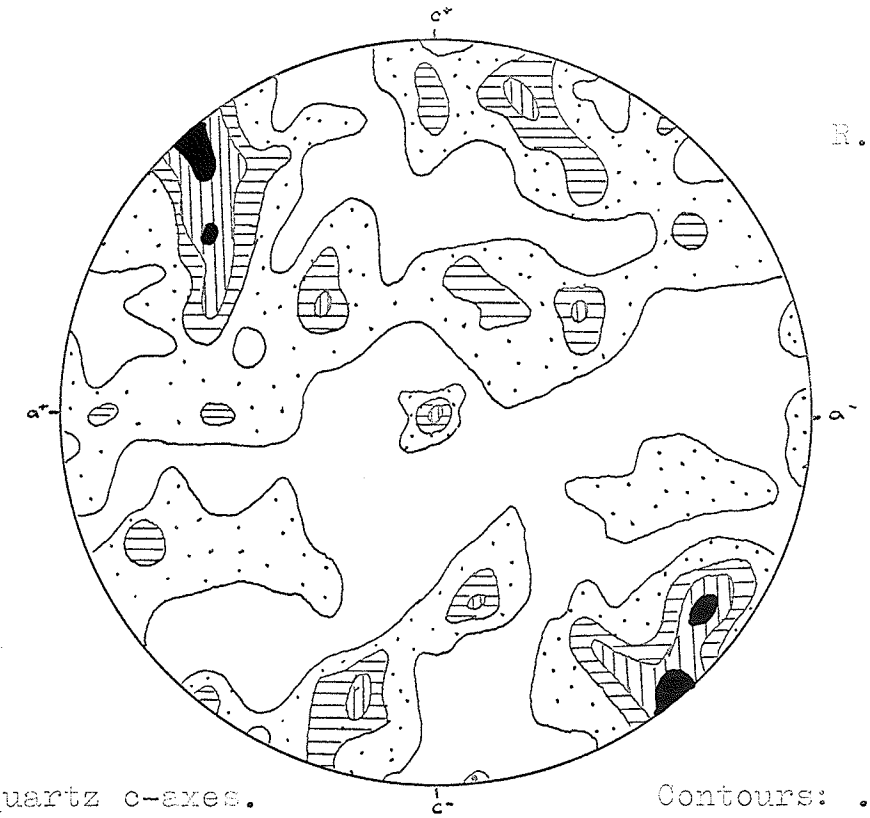

200 quartz c-axes. Contours: .75, I.75, 2.5, 3.5%.

Max. 4%.

Plate-22

A. R.R.-15

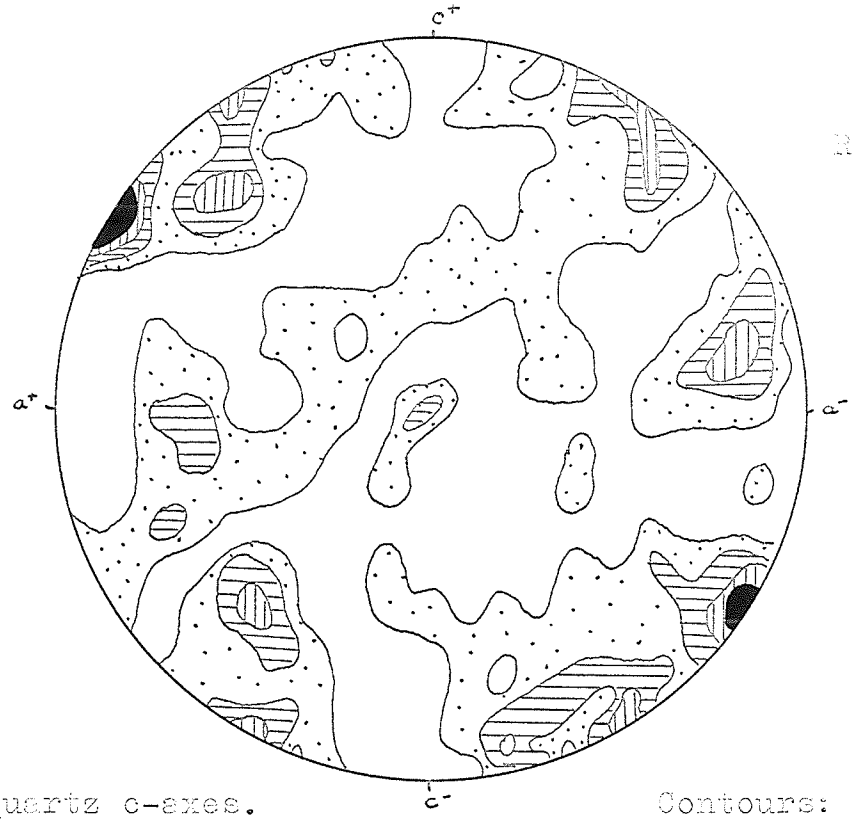

200 quartz c-axes. Contours: .75, 1.75, 2.5, 3.5%.

Max. 4%.

B. R.R.-20

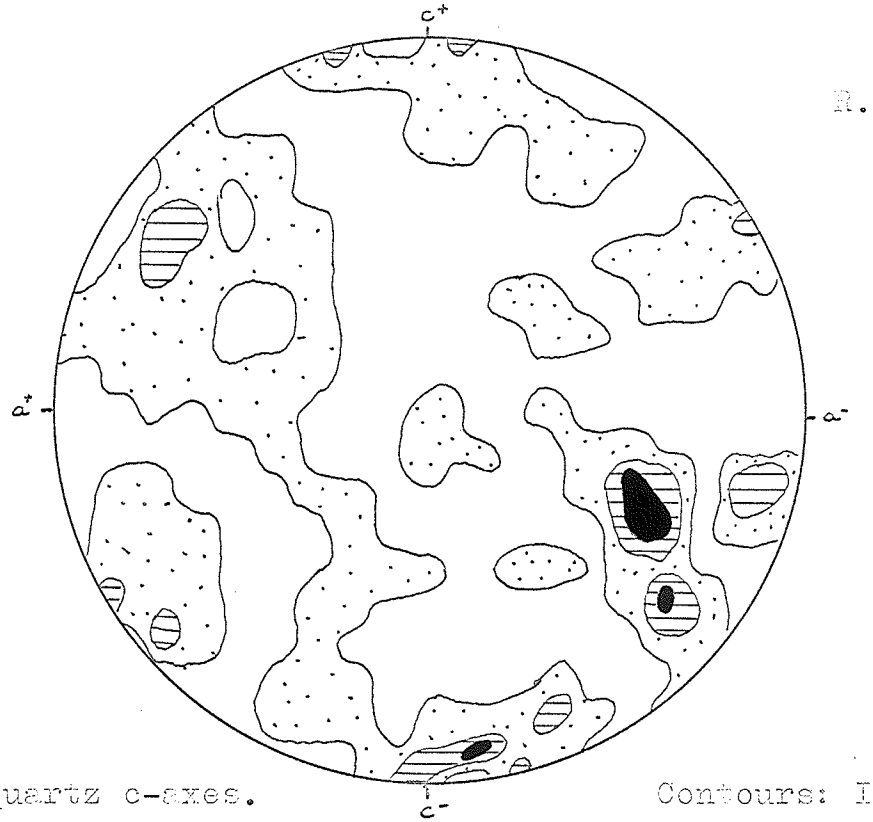

150 quartz c-axes. Contours: 1, 2, 3%.

Max. 3.3%.

Plate-23

A. R.R.-2I

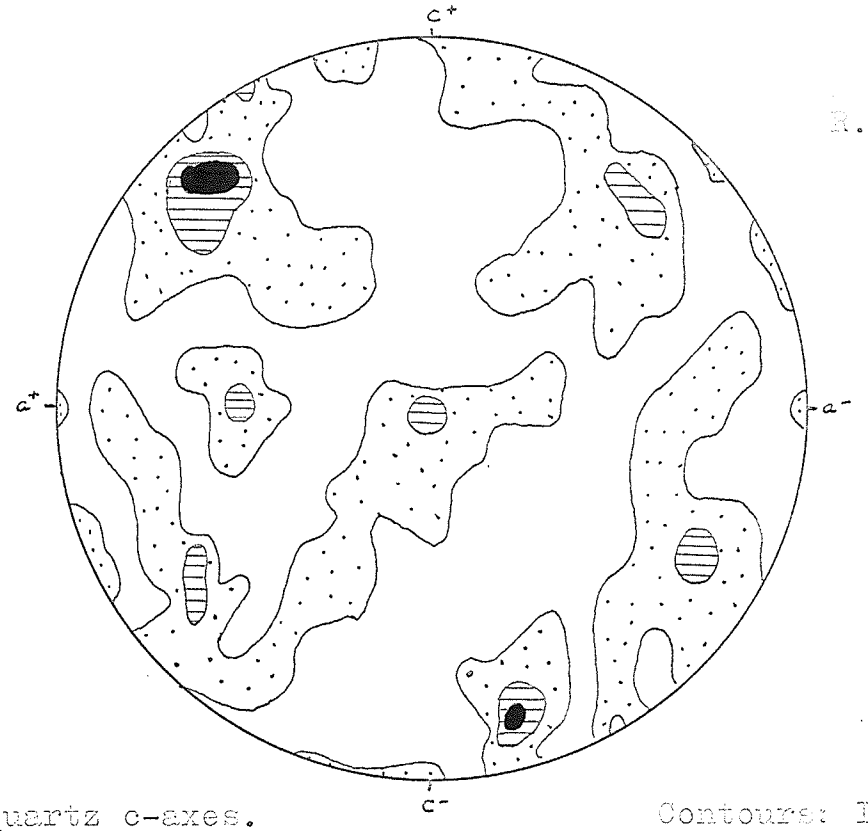

I50 quartz c-axes. Contours: I, 2, 3%.

Max. 3.3%.

B. R.R.-22

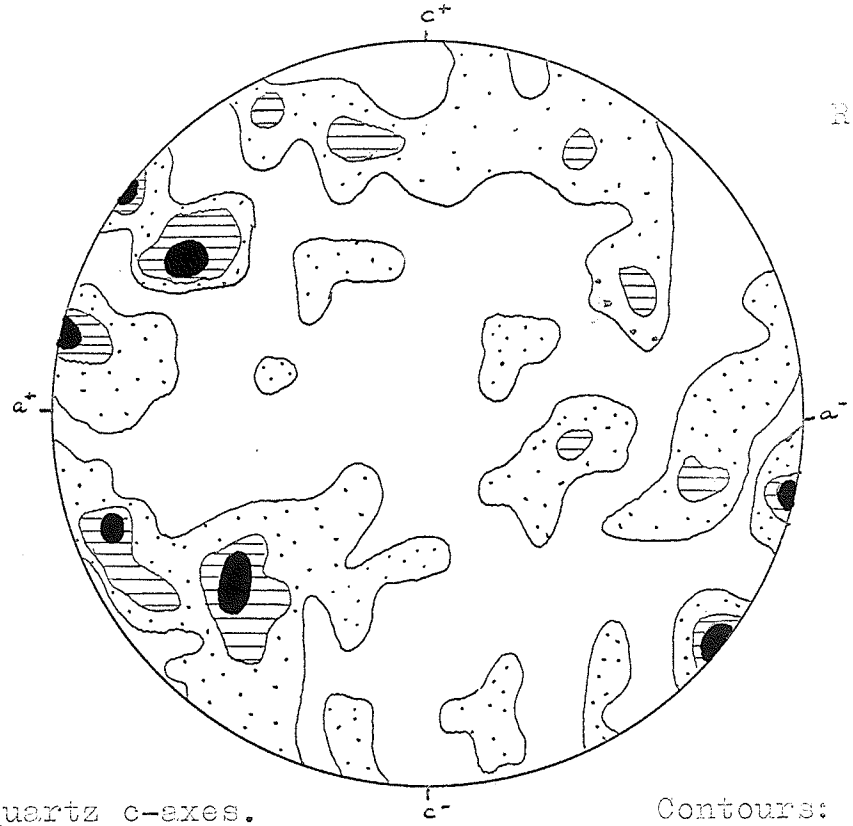

I50 quartz c-axes. Contours: I, 2, 3%.

Max. 3.9%.

Plate-24

A.

R.R.-23

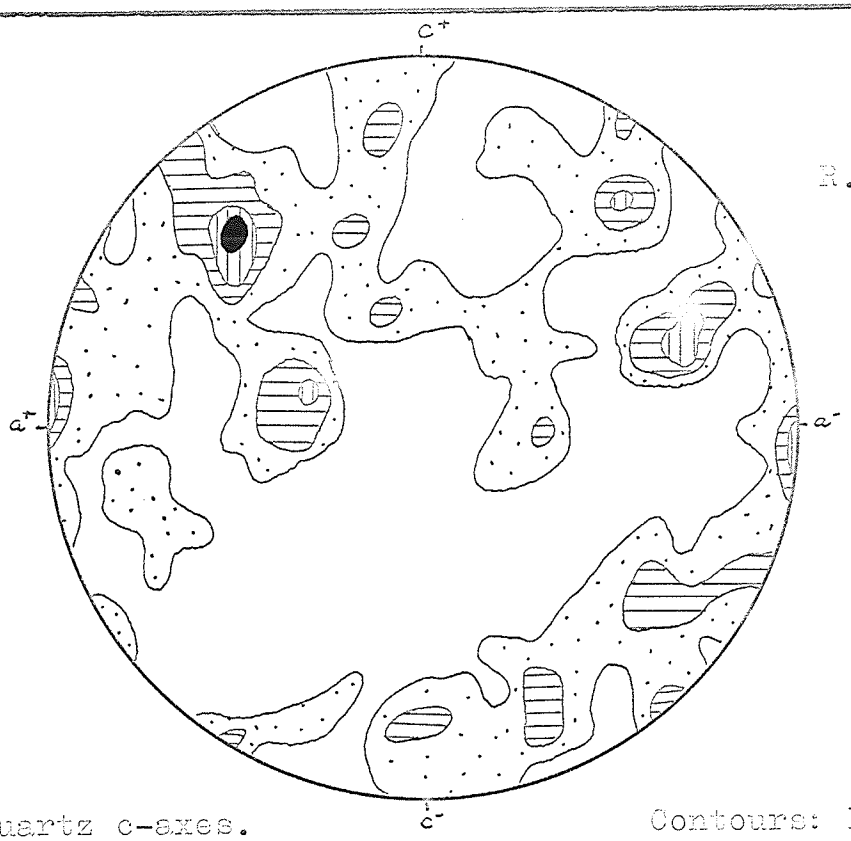

I72 quartz c-axes.

Contours: I, 2, 3, 4%.

Max. 4.6%.

B.

R.R.-47.

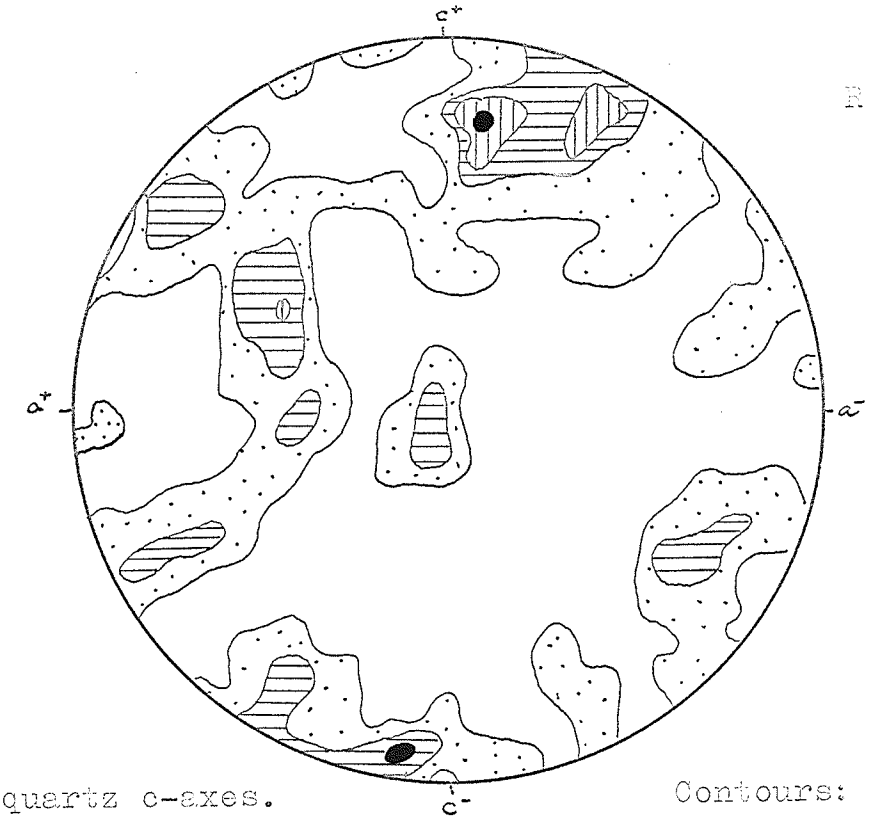

I50 quartz c-axes.

Contours: I, 2, 3, 4%.

Max. 4.6%.

Plate-25

A.

R.R.-24.

150 quartz c-axes.

Contours: 1, 2, 3, 4, 5%.

Max. 5.2%.

B.

R.R.-25

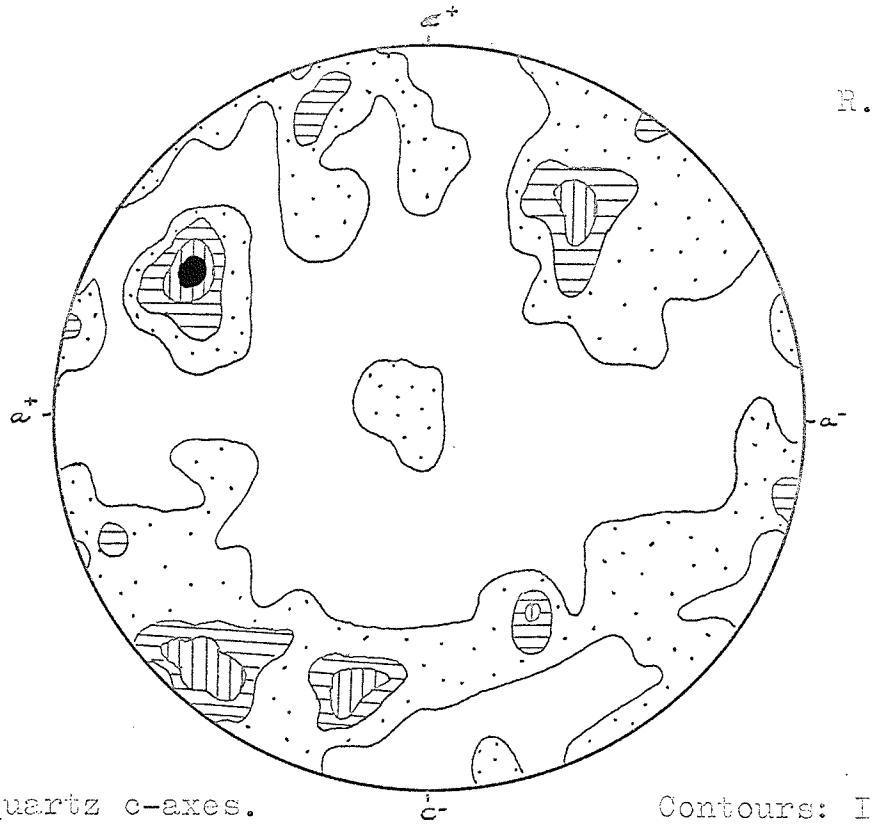

150 quartz c-axes.

Contours: 1, 2, 3, 4%.

Max. 4.5%.

Plate-26

A.

R.R.-26.

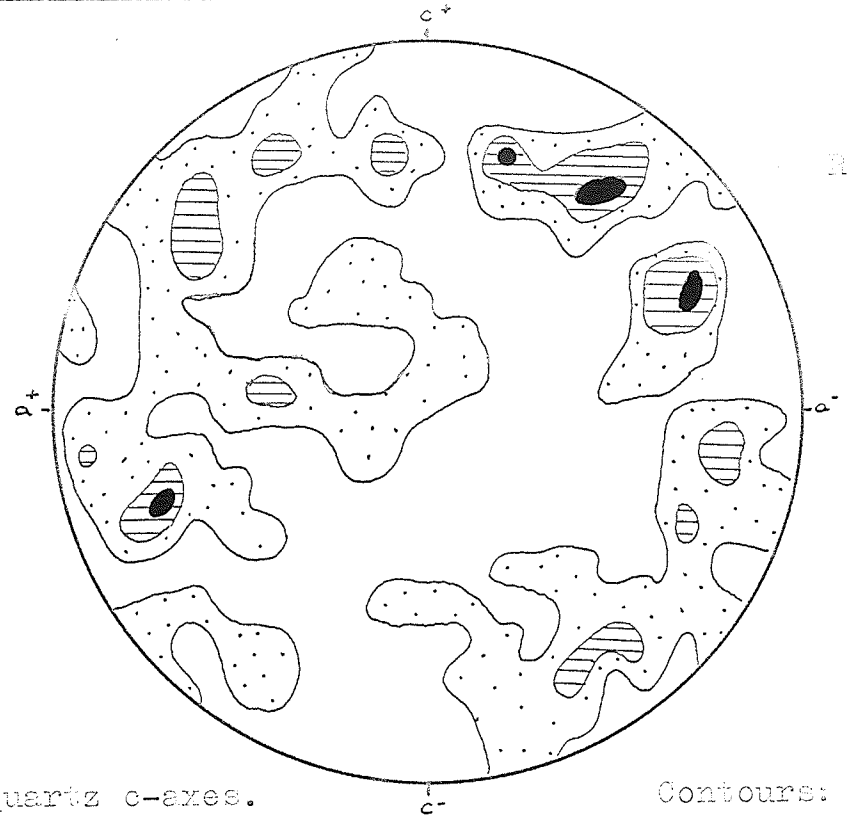

I50 quartz c-axes.

Contours: I, 2, 3%.

Max. 3.9%.

B.

R.R.-27

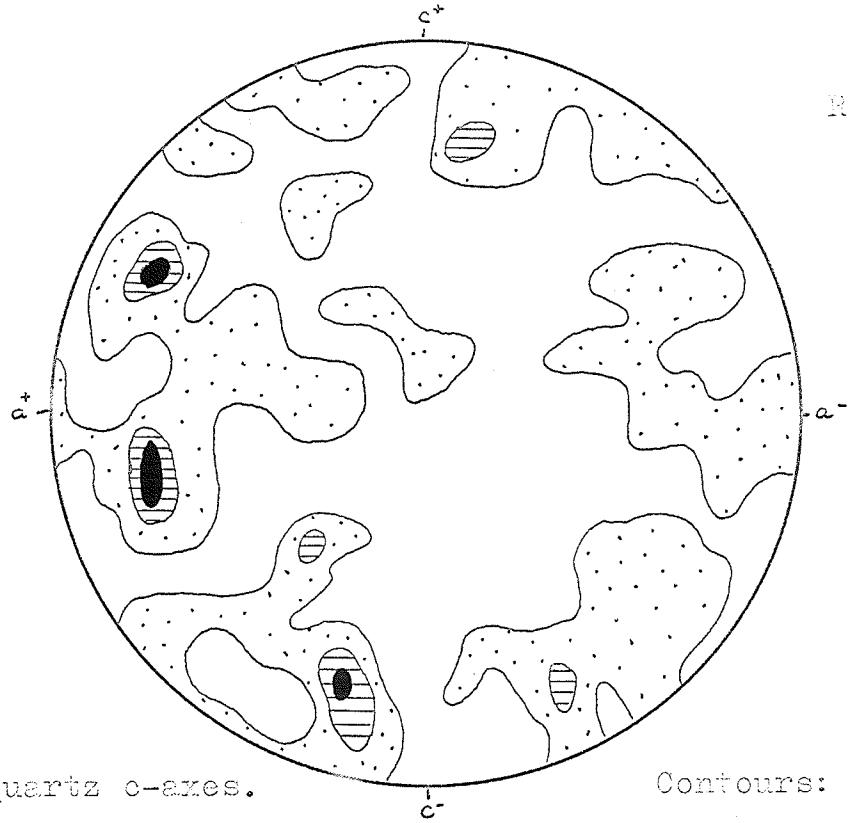

I50 quartz c-axes.

Contours: I, 2, 3%.

Max. 3.9%.

Plate-27

A.

R.R.-49

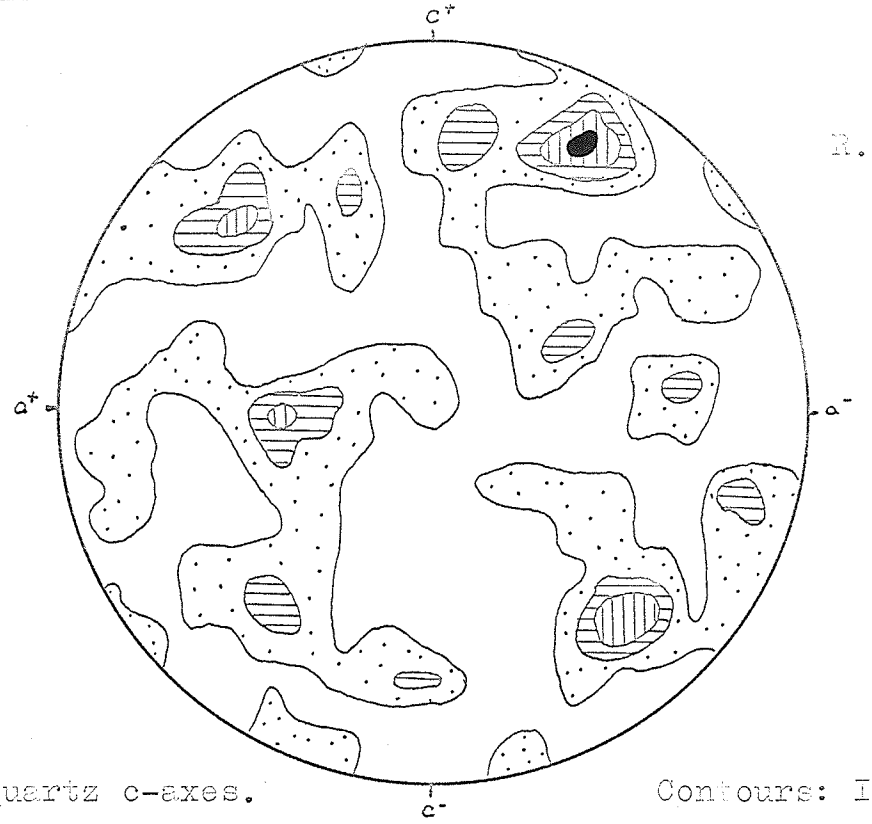

I50 quartz c-axes.

Contours: I,2,3,4%.

Max. 4.6%.

B.

R.R.-48

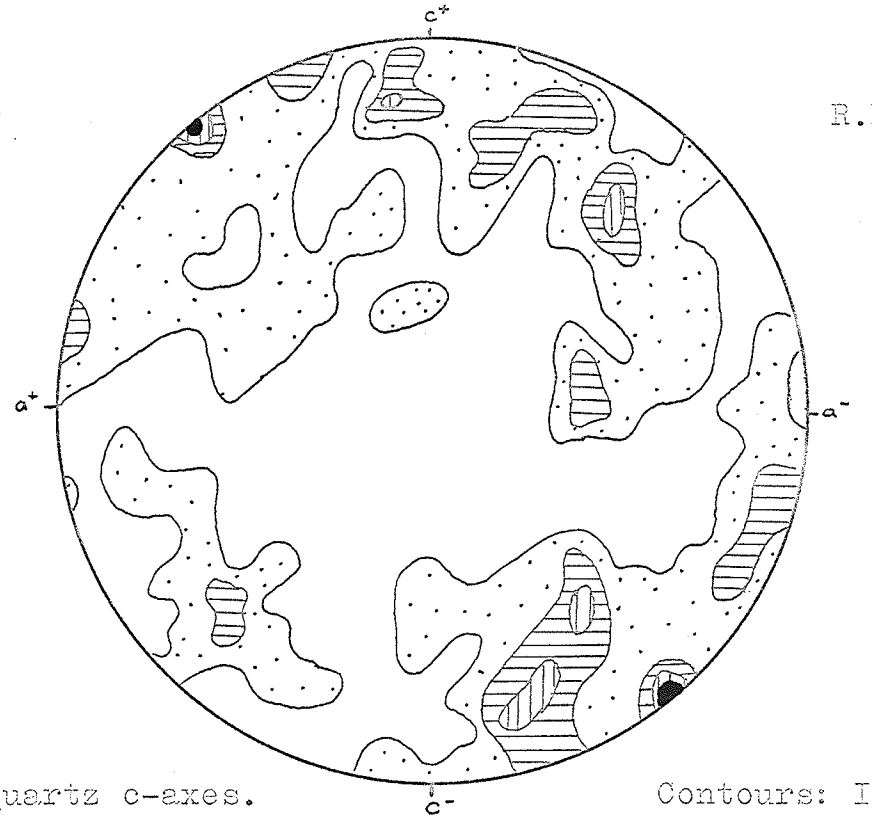

I50 quartz c-axes.

Contours: I,2,3,4%.

Max. 4.6%.

Plate-28

A. R.R.-46

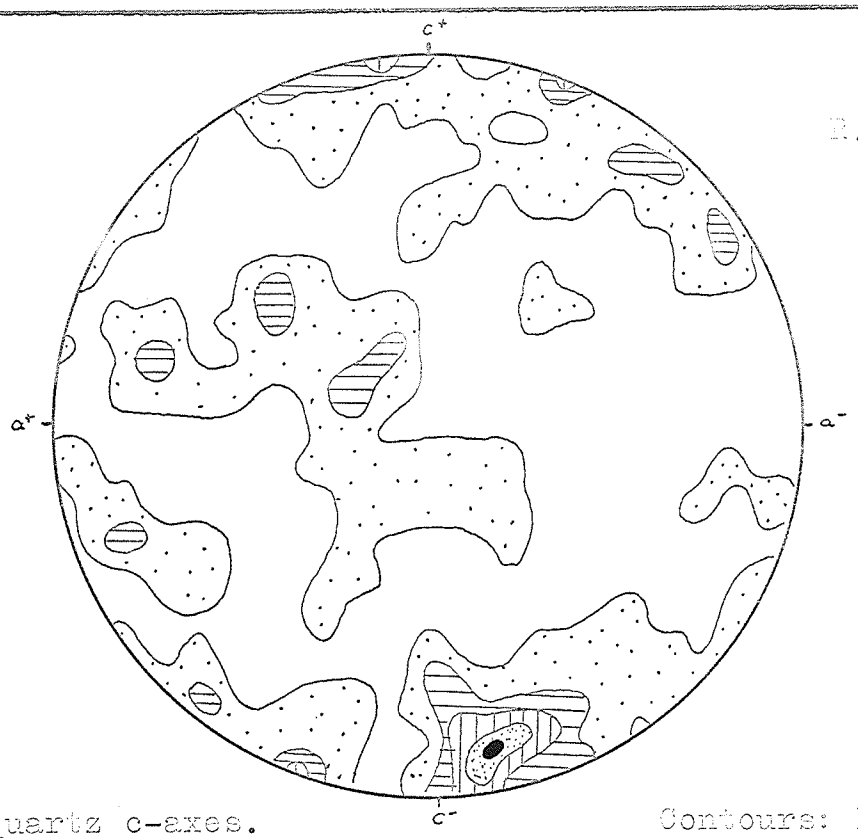

I50 quartz c-axes. Contours: I, 2, 3, 4, 5%.

Max. 5.2%.

B. R.R.-45

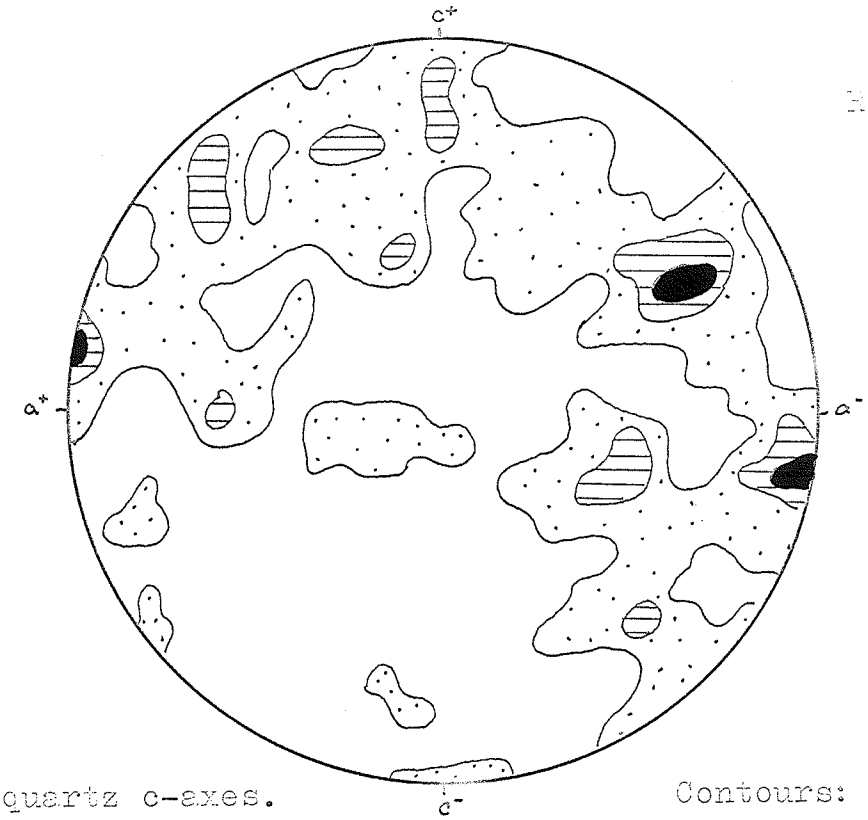

I55 quartz c-axes. Contours: I, 2, 3%.

Max. 3.78%.

Plate-29

A. R.R.-44

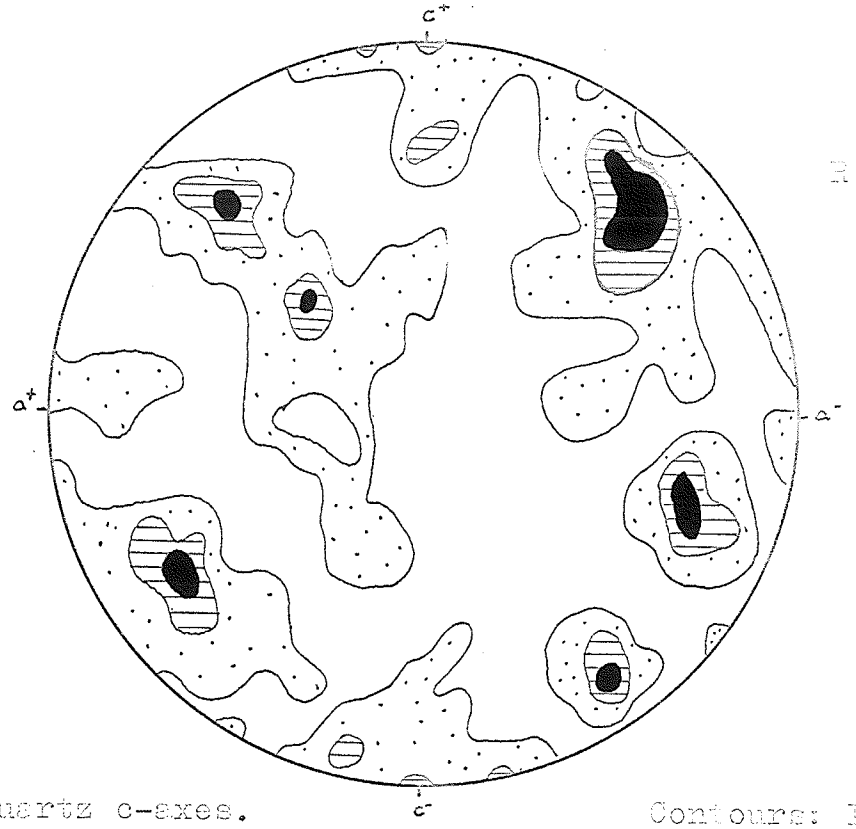

150 quartz c-axes. Contours: 1, 2, 3%.

Max. 3.9%.

B. R.R.-30

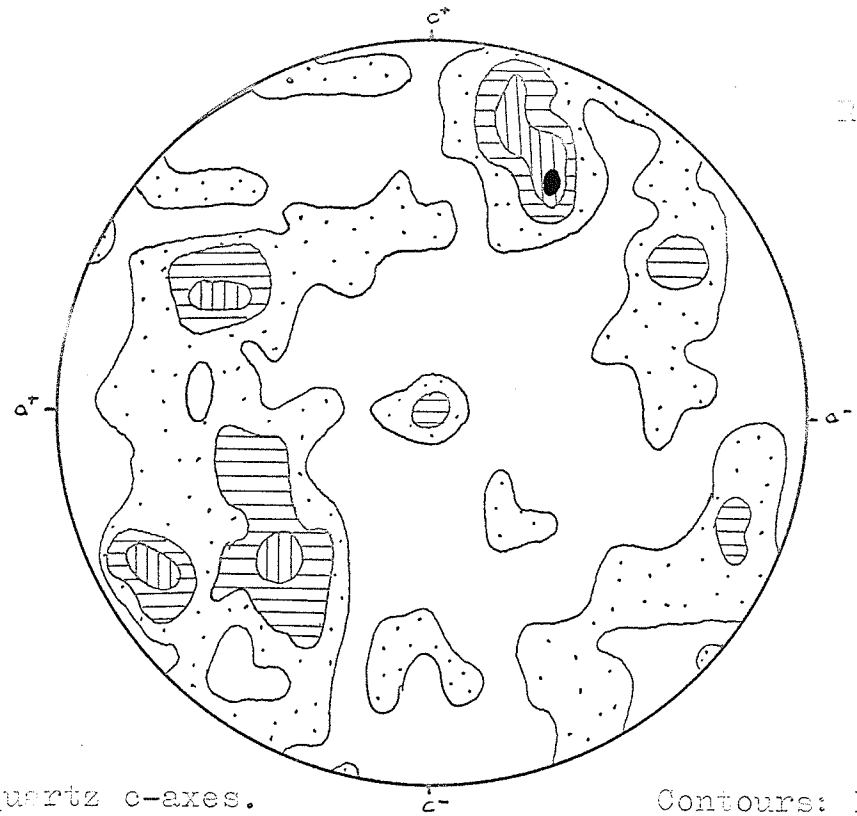

150 quartz c-axes. Contours: 1, 2, 3, 4%.

Max. 4.6%.

Plate-30

A. M.R.-3I

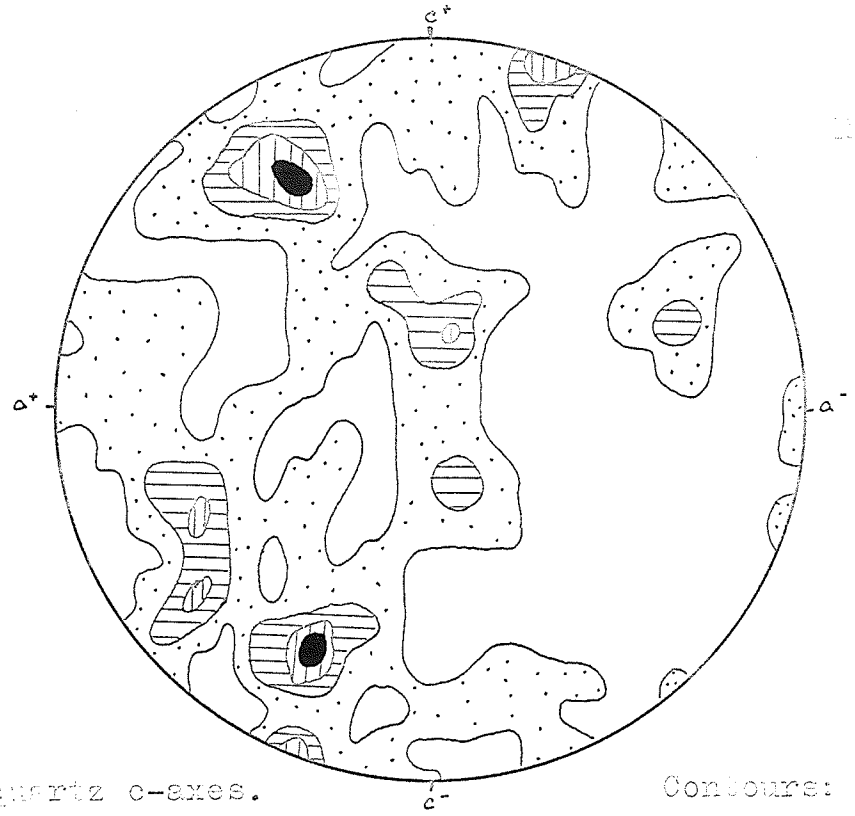

150 quartz c-axes. Contours: I, 2, 3, 4%.

Max. 4.6%.

B. M.R.-I

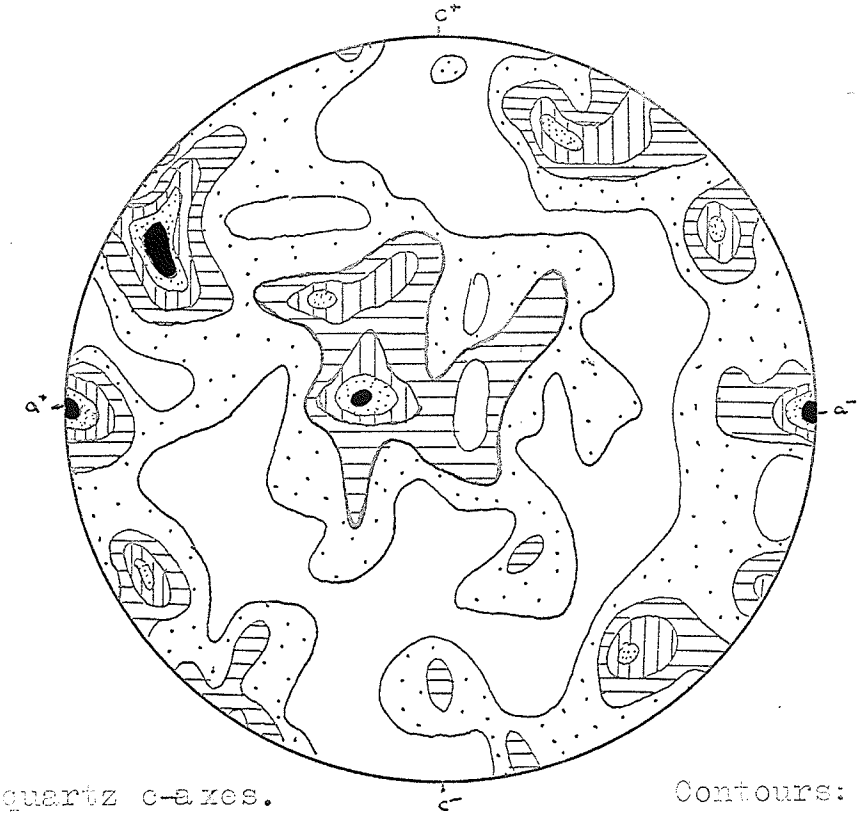

226 quartz c-axes. Contours: .5, I.5, 2, 2.5, 3%.

Max. 5.5%.

Plate-3I

A.

R.R.-2

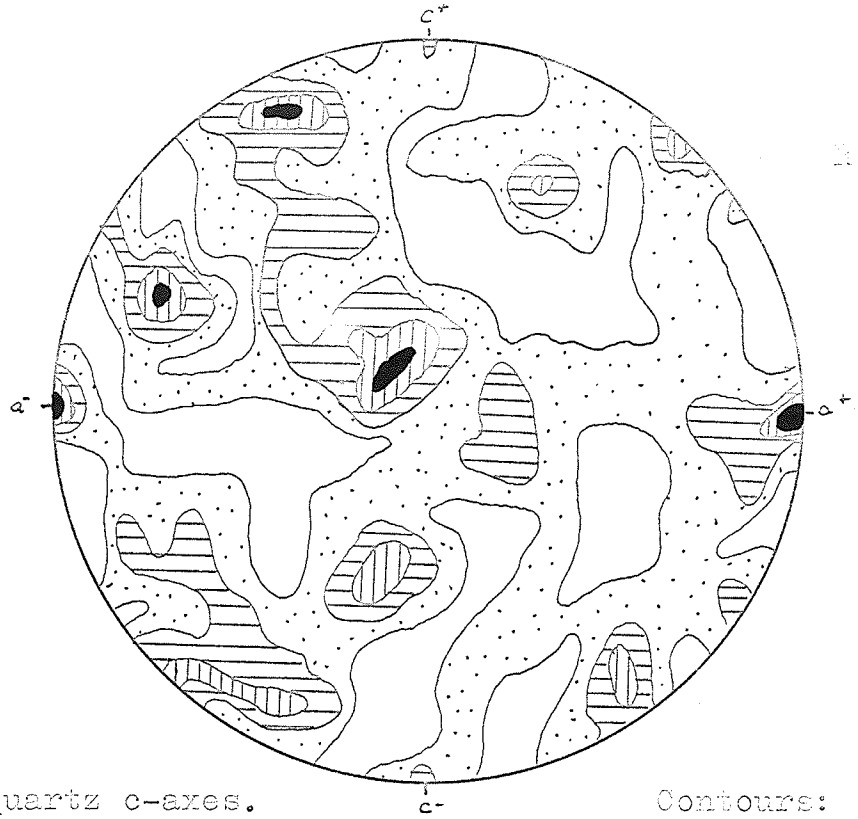

200 quartz c-axes.

Contours: .5,1.5,2.5, 3.5%.

Max. 5.5%.

B.

R.R.-3

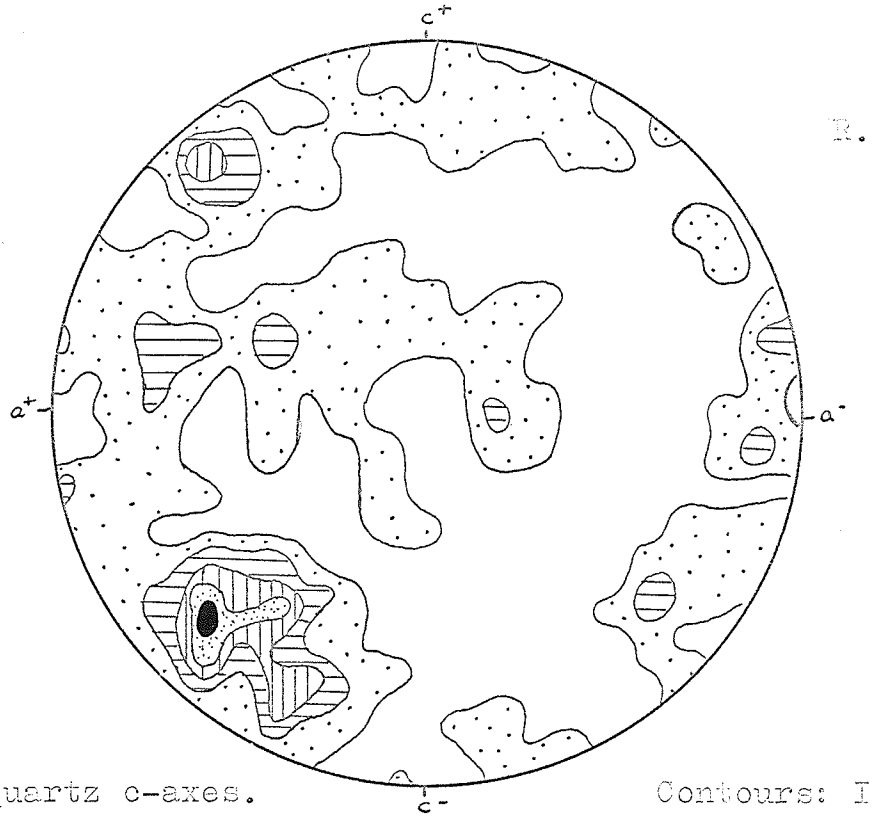

150 quartz c-axes.

Contours: 1,2,3,4,5%.

Max. 5.9%.

Plate-32

A.

R.R.-4

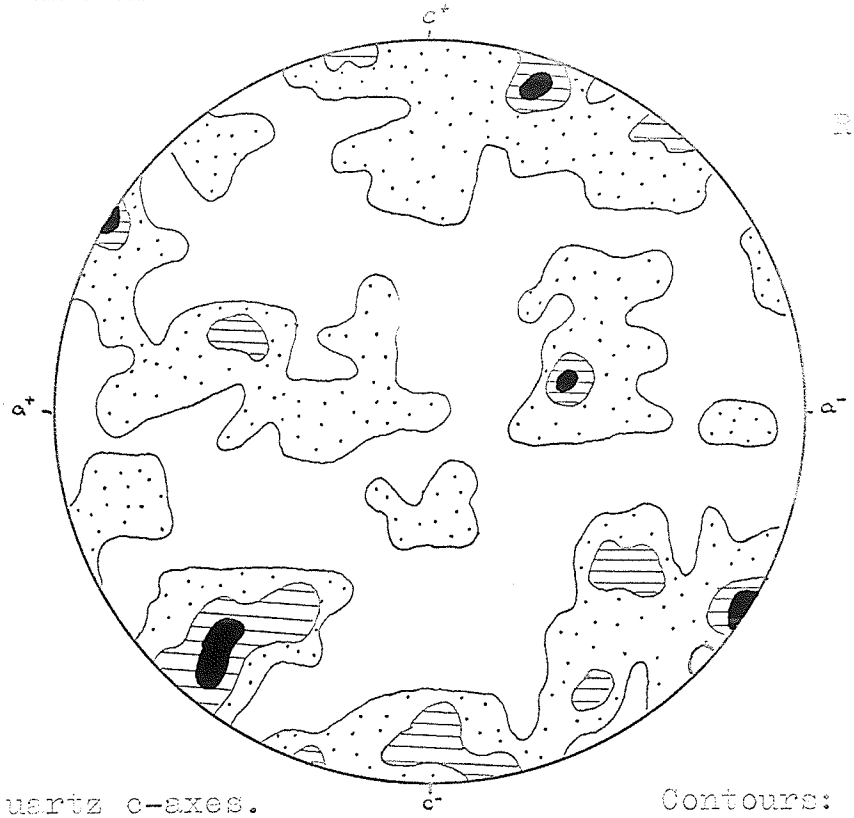

150 quartz c-axes.

Contours: 1, 2, 3%.

Max. 3.3%.

B.

R.R.-5

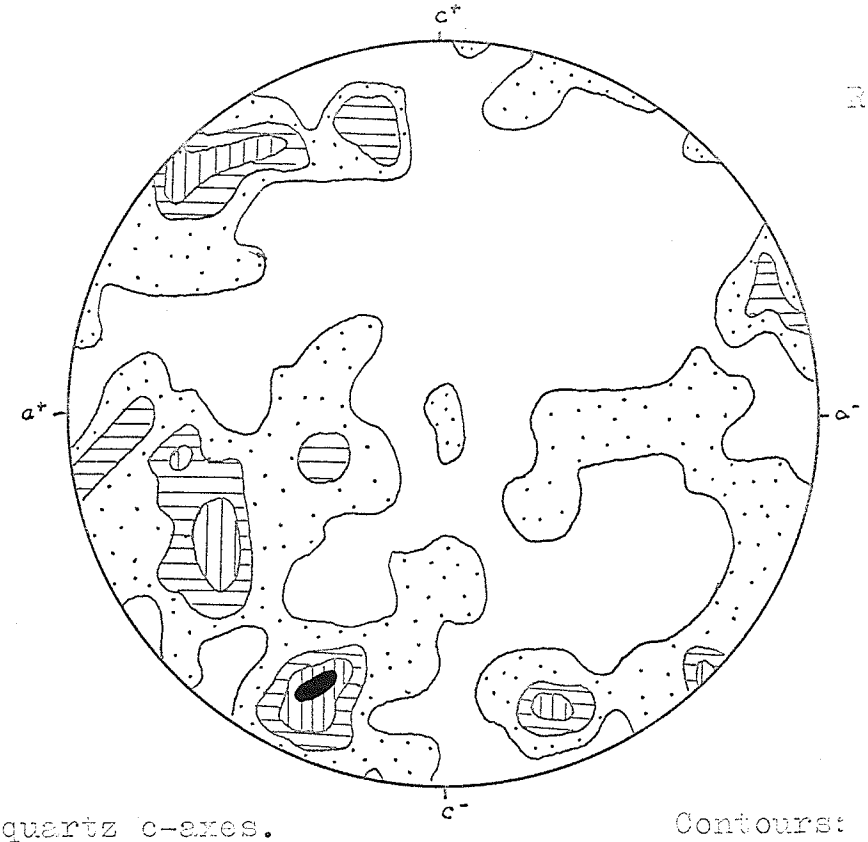

150 quartz c-axes.

Contours: 1, 2, 3, 4%.

Max. 4.8%.

Plate-33

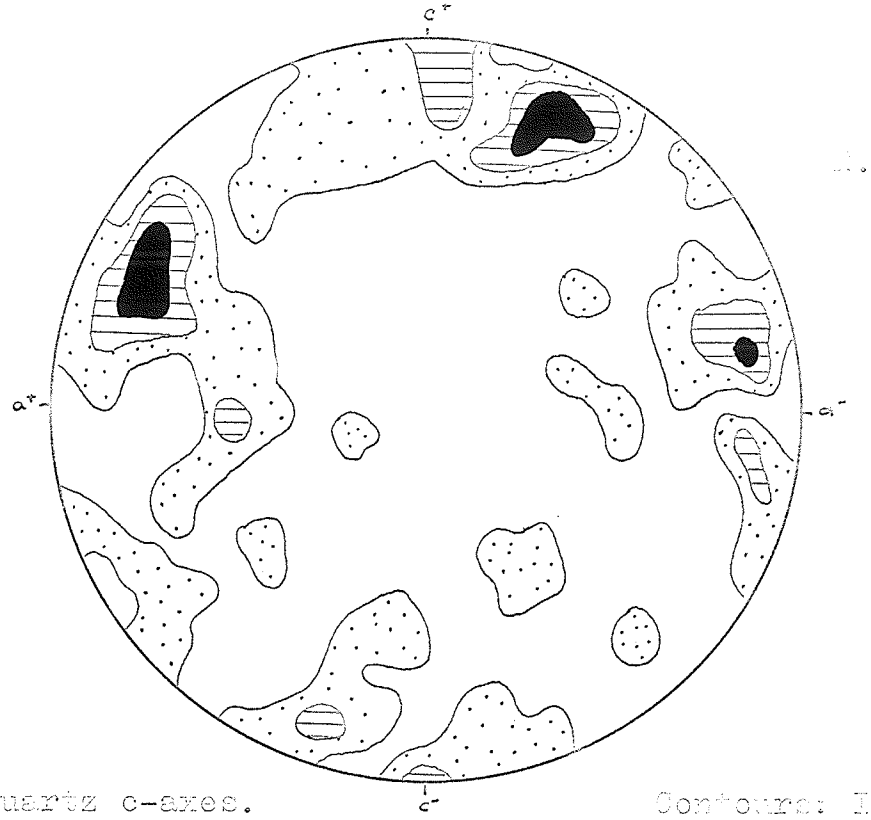

A. N.R.-5

150 quartz c-axes. Contours: 1, 2, 3%.

Max. 3.9%.

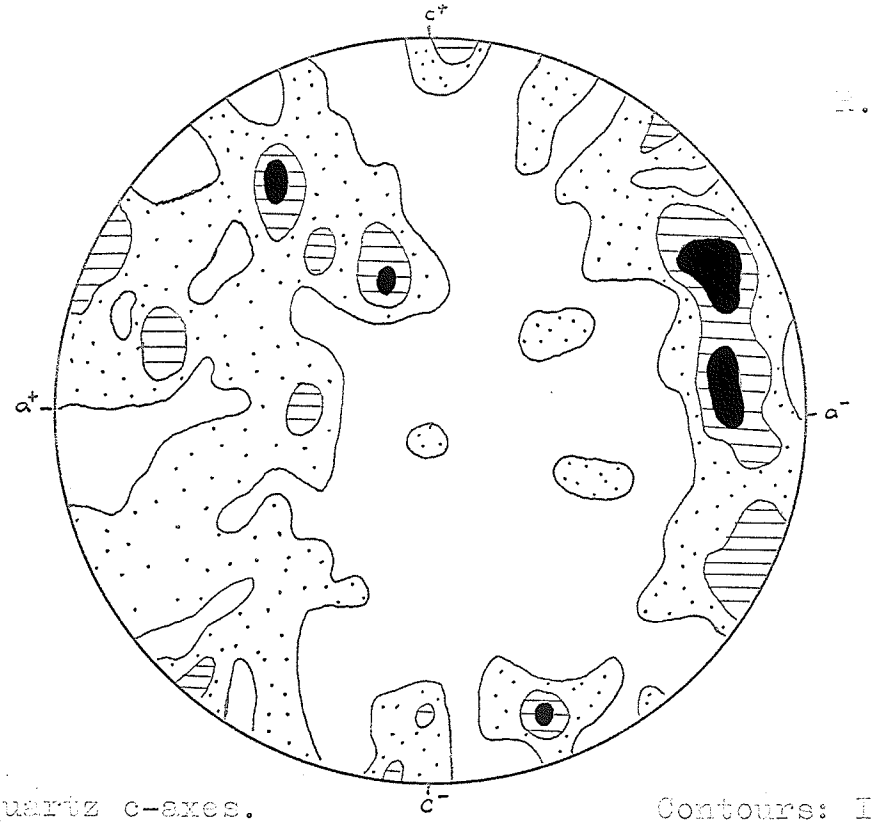

B. N.R.-7

150 quartz c-axes. Contours: 1, 2, 3%.

Max. 3.3%.

A.

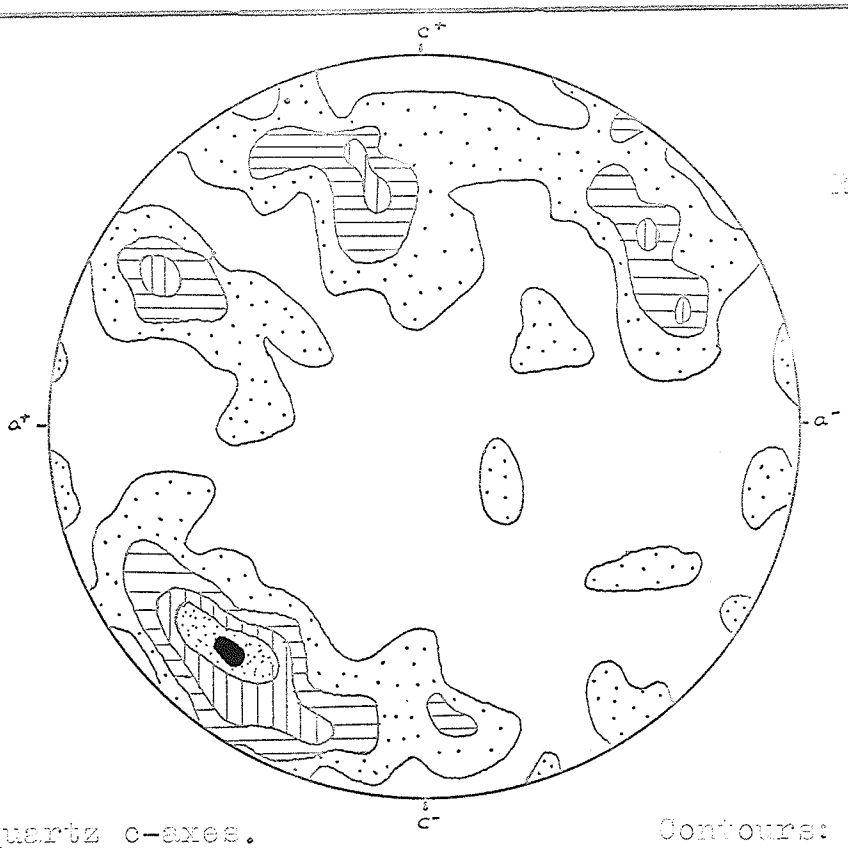

M.R.-36

150 quartz c-axes.

Contours: 1, 2, 3, 4, 5%.

Max. 5.0%.

B.

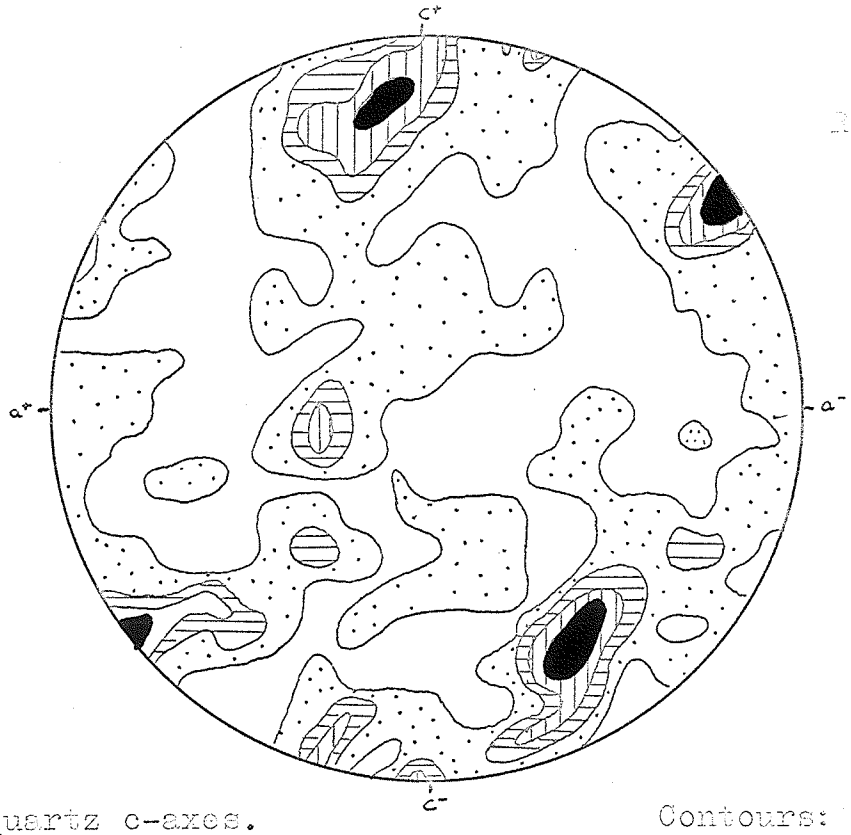

M.R.-8

200 quartz c-axes.

Contours: .75, 1.75, 2.00, 2.75%.

Max. 3.5%.

Plate-35

R.R.-10

200 quartz c-axes.

Contours: .75, 1.75, 2.5, 3.5%.

Max. 4%.

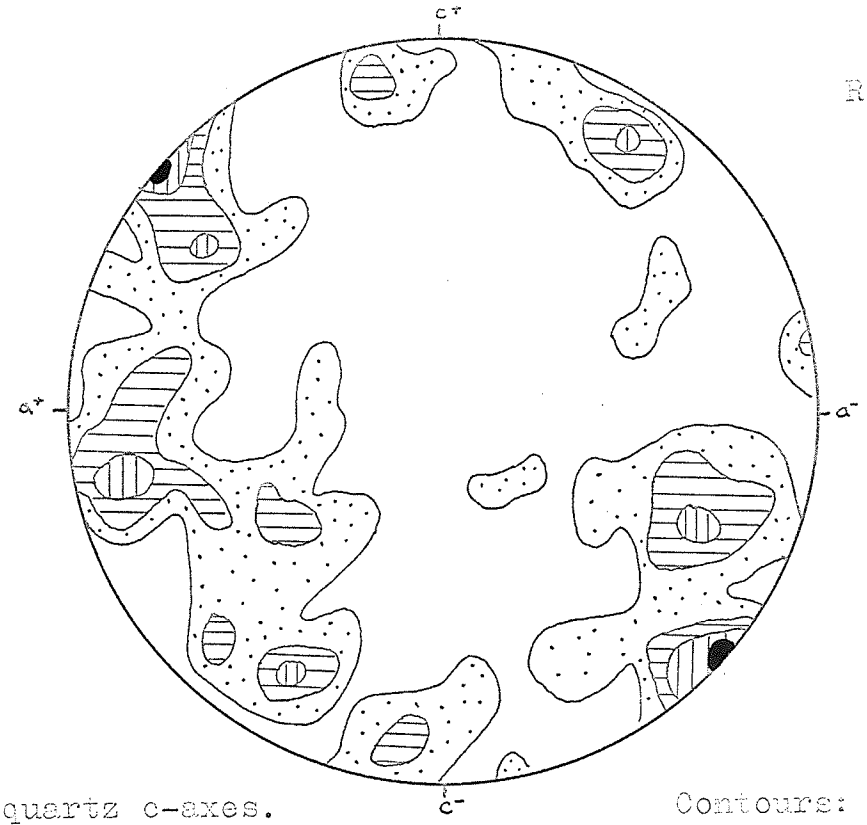

B.

R.R.-11

150 quartz c-axes.

Contours: 1, 2, 3, 4%.

Max. 4.4%.

Plate-36

A. R.R.-4I

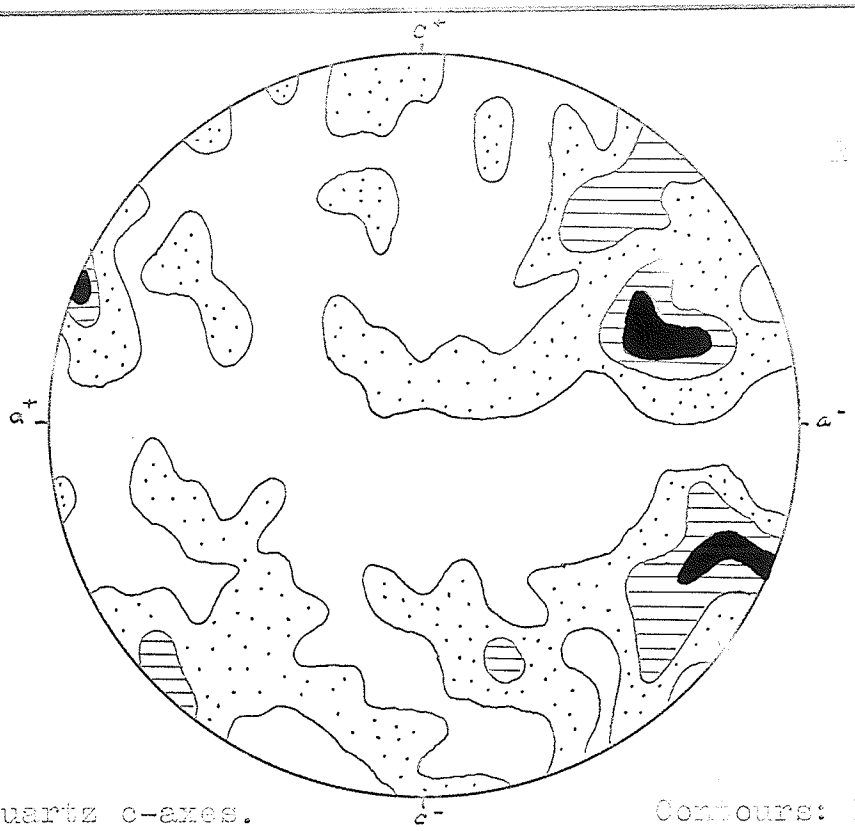

150 quartz c-axes. Contours: I, 2, 3%.

Max. 3.9%.

B. R.R.-I2

200 quartz c-axes. Contours: .75, I.75, 2.5, 3.5%.

Max. 4%.

Plate-37

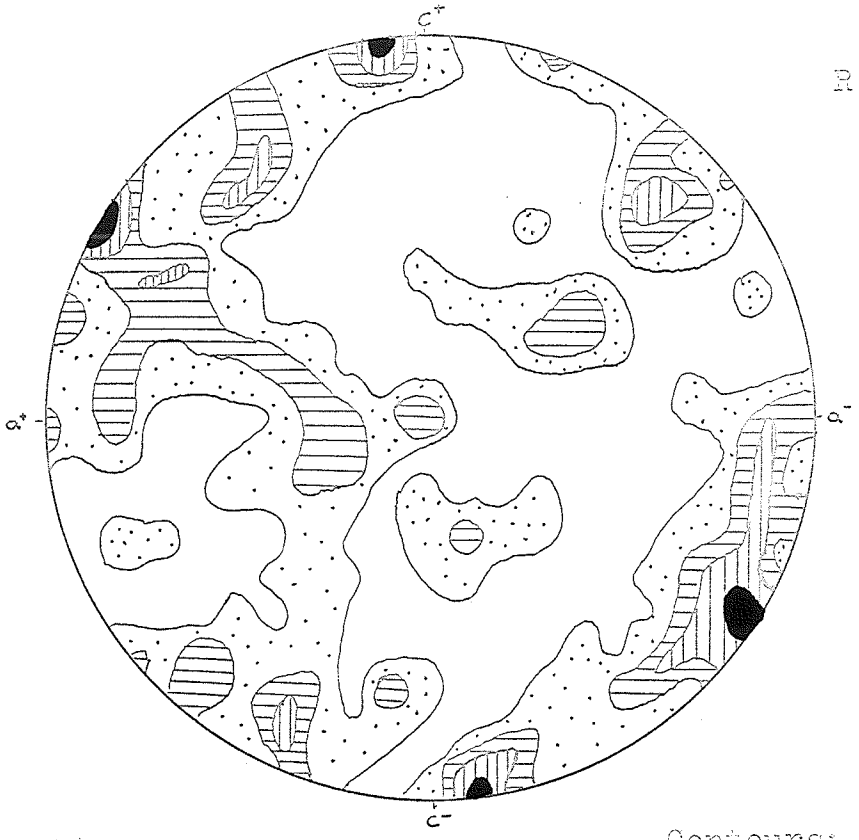

R.R.-I4

200 quartz c-axes.

Contours: .75, I.75, 2.5, 3.5%.

Max. 4%.

Plate-38

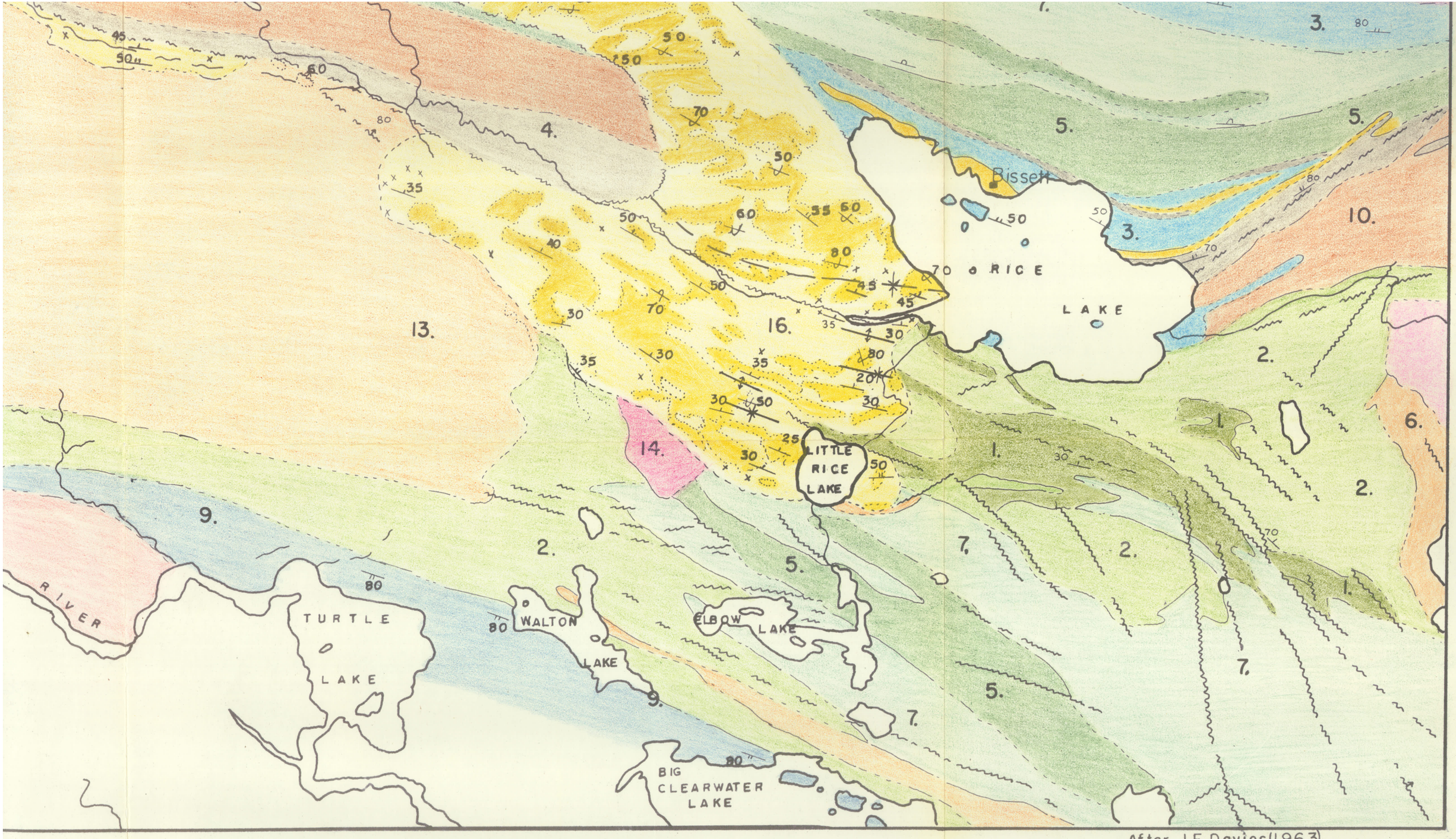

GEOLOGY OF THE

RICE LAKE AREA

MANITOBA

miles 1/8 3/4 4/8 1/2 0 1 1 1/2 2 miles

After J.F. Davies, (1963)

Fig.6

RICE LAKE GR

5 Dacite crystal tuff

4 Basalt, chlorite schist

3 Bedded tuff, lapilli tuff, arkose, conglomerate

2 Rhyolite; minor rhyolite breccia

1 Porphyritic dacite breccia

SYMBOLS

Area of rock outcrop, small outcrop.

Geological boundary, defined, approximate.

Bedding, direction of top unknown.

Bedding, direction of top known, beds upright.

Direction of top known, direction of dip unknown.

Bedding, overturned.

Anticlinal axis.

Synclinal axis.

Fault or shear zone, defined, assumed.

N
magnetic north
7°E

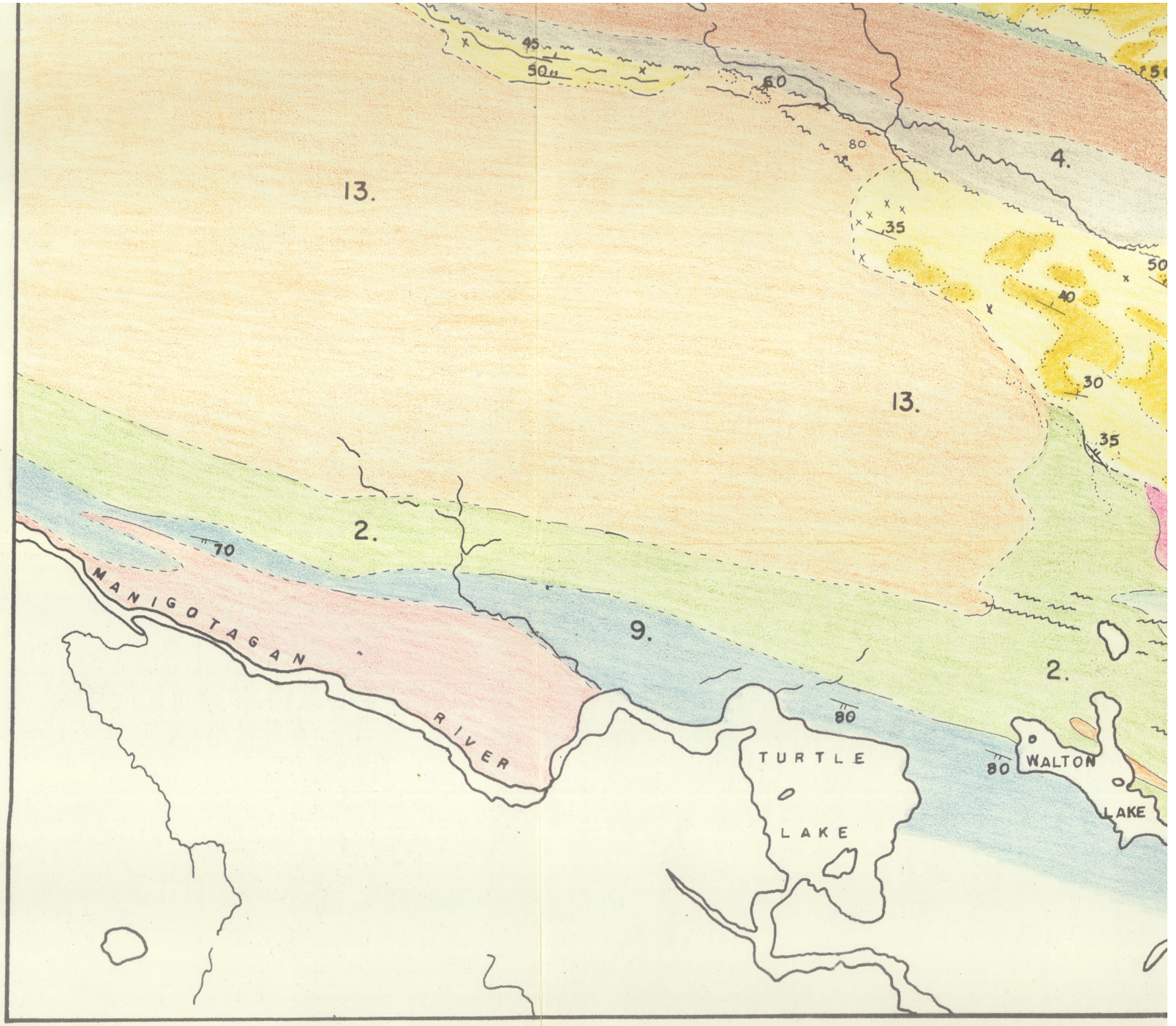

GEOLOGY OF
RICE LAKE
MANITOBA

miles 1/8 3/4 4/8 1/2 0

Fig.6

WOODS LAKE

4.

4.

W 80 RIVER

65

80

80

8.

80

16.

80

80

85

80

65

80

80

85

70

80

85

70

75

HORSESHOE

70

60

LAKE

70

75

60

ROUND LAKE

80

17.

80

70

70

80

80

70

8.

80

80

14.

7.

3.

80

45

50

60

50

50

70

50

4.

5.

5.

80

Bissett

LEGEND

Precambrian

17 Microline granite, granodiorite (gneissic trend lines ~)

SAN ANTONIO FORMATION

16 Feldspathic quartzite, conglomerate (ooo)

CALCIC INTRUSIVE ROCKS

15 Peridotite

14 Quartz-feldspar porphyry

13 Quartz diorite

12 "Quartz-eye granite"

11 Diabase

10 Gabbro

PRINCE LAKE GROUP

9 Quartz-feldspar-mica schist and gneiss

8 Subgreywacke, greywacke, slate

7 Dacite breccia, trachyte breccia

6 Porphyritic dacite

5 Dacite crystal tuff

4 Basalt, chlorite schist

3 Bedded tuff, lapilli tuff, arkose, conglomerate